Science of the Total Environment 798 (2021) 149313

Contents lists available at ScienceDirect

Science of the Total Environment

journal homepage: www.elsevier.com/locate/scitotenv

Are green roofs the path to clean air and low carbon cities?

S. Rafael *, L.P. Correia, A. Ascenso, B. Augusto, D. Lopes, A.I. Miranda

CESAM, Department of Environment and Planning, University of Aveiro, 3810-193 Aveiro, Portugal

HIGHLIGHTS

- Green roofs (GR) are seen as an opportunity to deal with cities air pollution.
- Two GR scenarios were studied using the WRF-SLUCM-CHIMERE modelling setup.
- The direct effect of GR revealed both positive and negative impact on air quality.
- GR promotes a reduction of the buildings energy needs and its related emissions.
- Decision makers need to be supported based on green roofs' multipurpose assessment.

GRAPHICAL ABSTRACT

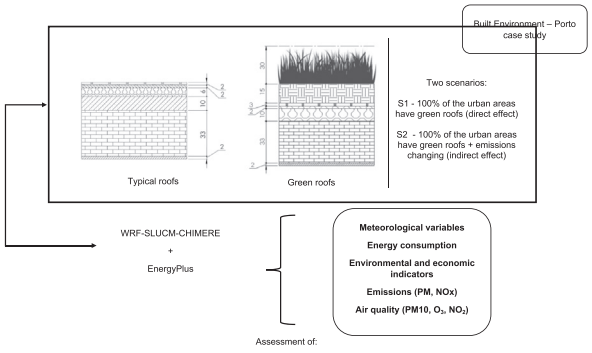

ARTICLE INFO

Article history:
Received 24 May 2021
Received in revised form 23 July 2021
Accepted 23 July 2021
Available online 30 July 2021

Editor: Jay Gan

Keywords:
Green roofs
Air quality
Atmospheric emissions
Energy savings
Thermal comfort
Numerical modelling

ABSTRACT

Green roofs, as part of urban green structures, have been pointed out as the solution to pursuit the goal of healthy cities. This study aims to investigate the direct, focused on meteorological changes, and indirect, related to both meteorological and emissions changes, impacts of green roofs on air quality (PM10, NO_2 and O_3). For that, the numerical modelling system composed by the WRF-SLUCM-CHIMERE models was applied to a 1-year period (2017), having as case study the Porto urban area. The EnergyPlus model was also applied to estimate the green roofs impacts on the building's energy needs and related impacts on air quality and atmospheric emissions. The analysis of the direct impacts showed that green roofs promote a temperature increase during the autumn and winter seasons and a temperature decrease during the spring and summer seasons. Both negative - concentrations increase - and positive - concentrations decrease - impacts were obtained for the primary, PM10 and NO_2, and secondary, O_3, air pollutants, respectively, due to changes in the dynamical structure of the urban boundary layer. The indirect effects of green roofs showed their potential to enhance the buildings energy efficiency, reducing the cooling and heating needs. These changes in energy consumption promoted an overall decrease of the environmental and economic indicators. Regarding air quality, the impact was negligible. The obtained results highlight the need for a multipurpose evaluation of the impacts of green roofs, with the different effects having to be traded off against each other to better support the decision-making process.

1. Introduction

Cities have an important role to play in pushing forward environmental change (EU (European Union) and UN-HABITAT (United Nations Human Settlements Programme), 2016). They stand as a hub of economic growth, innovation, culture and creativity, and thus cities are facing pressures related to social, economic and environmental problems, such as overcrowding, air pollution and climate change effects (Alberti et al., 2019). Air pollution is one of the most important environmental problems affecting people's health, particularly in urban areas of Europe, where millions of European citizens are being exposed

* Corresponding author.
E-mail address: sandra.rafael@ua.pt (S. Rafael).

https://doi.org/10.1016/j.scitotenv.2021.149313
0048-9697/

to air pollutants that are above the European Union (EU) air quality standards and the more stringent World Health Organization (WHO) air quality guidelines. Nitrogen dioxide (NO_2), particulate matter (PM10 and PM2.5) and ozone (O_3) are still the main critical air pollutants (EEA, 2020). Climate change exacerbates air pollution problems, which combined with the increasing magnitude, duration and frequency of extreme climate events pose a significant threat to cities (Kaspersen and Halsnæs, 2017). At the same time, cities are responsible for around 80% of greenhouse gas (GHG) emissions, mostly related to energy consumption through the burning of fossil fuels for transport, energy in-use in buildings and appliances (Rafael et al., 2016). In fact, about 30% of GHG emissions through energy use are attributed to the buildings sector (Leal et al., 2019).

Technological solutions (i.e., enhanced abatement technology), soft-measures (i.e., nature-based solutions) and, more recently, behavioural changes (through citizen's engagement) have been implemented to deal with both air pollution and climate change challenges. The Roadmap for Carbon Neutrality 2050 (EC - European Commission, 2018), the EU R&I policy agenda on Nature-Based Solutions (NBS) (EC - European Commission, 2015), and the Europe Green Deal (EC - European Commission, 2019) set the framework and rationale for research, citizen science and policy action. To achieve the goal of the European Green Deal to pursuit a clean, greener, resilient and healthy city, interlinked solutions need to be explored to maximise benefits for health, quality of life and climate resilience. The European climate objectives for 2030 and 2050 are well aligned with the Sustainable Development Goals (SDG) that aim to make cities inclusive, safe, resilient and sustainable, and highlight the need to take urgent action to combat climate change and its impacts (SDG 11 and SDG13, respectively). The green roofs technique, which combines technology and nature in a single solution, can have the potential to turn these challenges into a unique opportunity.

Green roofs are vegetated surfaces, consisting of plants usually grown on particular substrate material on a building rooftop (Shafique et al., 2020). They offer to buildings and their surrounding environment many benefits (Castleton et al., 2010). Several studies have been reporting green roofs' environmental benefits, but the majority of them were focused on the effects in the city microclimate. Rafael et al. (2020a), Laloševic et al. (2018) and MacIvor et al. (2016) assessed the impact of vegetative roof systems on the urban environment showing that green roofs help reduce temperatures around buildings, between 0.1 and 6 °C, through increasing evapotranspiration process, and further decreasing building energy consumption (Sadineni et al., 2011). According to the studies compiled by Shafique et al. (2020), green roofs energy savings on heating and cooling processes can vary between 0.6 and 70%. A reduction in energy demand can further reduce GHG emissions from energy production (Jaffal et al., 2012) by reducing the burning of fossil fuels. Few studies have been analysing the impacts on air quality. Works such as Rafael et al. (2020a) and Fallmann et al. (2016) assessed the direct effects of green roofs on air quality under heat wave episodes, concluding that both positive and negative impacts can be found. However, the set of studies focused on air quality hardly ever evaluates the impacts of green roofs energy savings on air quality, the so-called indirect effect.

In this scope, there is a question that still needs to be explored: Are green roofs the path to clean air and low carbon cities? The main goal of this study is therefore to investigate and quantify the direct (local climate and air quality) and indirect (energy savings, carbon and air pollutant emissions) impacts of green roofs along a 1-year period, for the Porto urban area. Three urban air pollutants were analysed: PM10, NO_2 and O_3. This work is distinguishable from previous ones in three features: i) the majority of studies has been focused on one dimension of green roofs benefits without considering multipurpose features in cities; ii) the majority of studies has been focused on short periods' assessments (i.e., heat waves), without exploring the annual, seasonal and monthly patterns; iii) the few studies that analyse air quality were only focused on the direct impact of green roofs on air pollutant concentrations.

The paper is structured as followed: Section 2 briefly introduces the case study; Section 3 describes the applied models and their simulation configurations, as well as the modelling setup methodology. A description of the scenarios developed and assessed in this work is also presented in Section 3. The direct and indirect benefits of green roofs in the study area are analysed and discussed in Section 4. Conclusions follow in Section 5.

2. Porto's case study

The Porto urban area is located in the North region of Portugal and it is the second-largest Portuguese city and one of the major urban areas in South-western Europe. Over the last decades, Porto had a continuous urban expansion at rates much higher than population growth, which resulted in a massive urban footprint and recognized air quality problems (Rafael et al., 2018, 2020a). Currently, the Porto urban area, with around 1.8 million inhabitants, has an area of 2041 km^2 with a population density of 843 inhab·km^{-2} (INE – Instituto Nacional de Estatística (Statistics Portugal), 2011). Porto has a mixed temperate oceanic and Mediterranean climate, characterized by warm summers and mild winters. The average daytime temperatures are about 14 °C in the winter and 25 °C during the summer. The winter is usually rainy while in the summer rain is very rare (IPMA - Instituto Português do Mar e da Atmosfera (Meterology Institute), 2013).

The Porto urban area is predominantly covered by artificial surfaces, characterized by a mixed land use: commercial/industrial and residential areas. According to the Portuguese Statistics Institute (INE – Instituto Nacional de Estatística (Statistics Portugal), 2018), with a total of 418,038 buildings, 99% of them for residential purposes, the Porto urban area concentrates the largest proportion of the housing stock in Portugal, with 34.2% of buildings and 31.6% of households, in 2017. The Porto housing stock is characterized by 79% of buildings with one or two floors and a predominance (22.6%) of dwelling T3 typology (3 bedrooms in a total of 5 rooms). The average living area per room is around 20.4 m^2, with a total dwelling area per floor of 190 m^2. An average number of 2.7 residents per dwelling was observed in 2017 (INE – Instituto Nacional de Estatística (Statistics Portugal), 2018). Regarding construction methods, the most commonly used building solutions, especially in residential buildings, have remained practically unchanged for several years. The construction system is well-rooted and is used throughout the country, usually consisting of a porticoes structure with pillars and beams in reinforced concrete and lightened slabs. For the execution of the outer walls, a simple wall solution, also in ceramic brick, is currently used (OERCO2 - Online Educational Resource for Innovative Study of Construction Materials Life Cycle, 2017). Almost half of the residential buildings had reinforced concrete structures (48.6%) and roughly one-third of the buildings had masonry walls with reinforced concrete slabs (31.7%). The remaining buildings had less representative structure types such as masonry walls without reinforced concrete slabs (13.6%), loose stone or adobe masonry walls (5.3%) and other types of structure (0.8%). With a strong prevalence of residential areas, the sector is responsible for 18% of the total energy consumption in the Porto urban area (PORDATA (Base de dados Portugal Contemporâneo), 2020a). 66% of the energy demand is linked to cooking activities, heating and cooling needs, and for lighting (INE – Instituto Nacional de Estatística (Statistics Portugal), 2011).

Due to its dimension and economic activities (e.g. maritime port, airport and oil refinery), the Porto urban area has been facing air quality problems. After a reducing trend of around 40% in the annual PM10 and NO_2 concentrations during the economic crisis (2007–2015) (Monteiro et al., 2018), an increase of annual average values of air pollutants concentrations has been observed since 2017 (Rafael et al., 2020a). According to Rafael et al. (2020a), the most critical pollutants in Porto urban area are NO_2 and PM10, with road traffic and residential

combustion, for NO_2 and PM10, respectively, as the main emitting sectors. The current and projected trends of air quality and climate (Rafael et al., 2020a; Sá et al., 2016; Carvalho et al., 2017), together with the importance of housing stock to energy consumption, make this city an interesting and challenging case study to evaluate the potentialities of green roofs.

3. Material and methods

A specific methodology was applied to assess the direct and indirect impacts of green roofs in the Porto urban area. Two main steps were performed: i) definition of the modelling setup (Section 3.1); and ii) design and characterization of scenarios (Section 3.2). To an easy understanding of the applied methodology, Fig. 1 illustrates the procedure followed in this study.

The direct impact assessment (S1) aimed to assess the impacts of green roofs on air quality (only) related to changes in local meteorology. For that, the modelling setup composed by the WRF-SLUCM-CHIMERE was applied. The indirect impact assessment (S2) aimed to investigate the impacts of green roofs on air quality based on the combined effects of the meteorology and of the atmospheric emissions (linked to buildings' energy savings). For that, the EnergyPlus model was added to the cascade of models to firstly assess the role of green roofs in the buildings' energy needs. The related changes in the atmospheric emissions were then used as input data in the WRF-SLUM-CHIMERE system to assess the air quality impacts. A complete description of the methodology used is given as follows.

3.1. Modelling setup

3.1.1. Air quality setup

The modelling system composed by the WRF-SLUCM-CHIMERE models was applied to one year simulation (2017). The Weather Research and Forecasting (WRF) model (Skamarock et al., 2008), version 3.7, coupled with the Single-Layer Urban Canopy Model (SLUCM) (Kusaka et al., 2001; Kusaka and Kimura, 2004), was used. The SLUCM is available as a WRF model module, in which coupling is made through the Noah Land Surface Model, to better represent the physical processes involved in the exchange of heat, momentum, and water vapour in an urban environment. This cross-scale atmospheric modelling system has been widely applied to both meteorology and air quality analysis when more accurate predictions for urban regions are required (Carvalho et al., 2017; Rafael et al., 2019, 2020a). The SLUCM consists of two-dimensional, symmetrical street canyons with simplified geometry of the buildings. Some of the features of the SLUCM include shadowing from buildings, reflection of short and longwave radiation, wind profile in the canopy layer and multi-layer heat transfer equation for roof, wall and road surfaces (Kusaka et al., 2001). The SLUCM requires inputs of urban canopy features such as building and trees height, roof and road width, percentage of impervious and vegetated surfaces, and thermal properties of building material. A detailed description of the WRF urban modelling system can be found in Chen et al. (2011). Rafael et al. (2019) investigated the best set of urban parameterizations for the study area, which were applied in this work (see Table S1 in the supplementary material).

The WRF-SLUCM was set up with three domains (see Fig. S1 in the supplementary material). The outer domain (D1), covers Europe and part of North of Africa and has 210 × 185 horizontal grid cells with a horizontal resolution of 25 km; the nested domain D2 includes the Portugal mainland and has 131 × 176 horizontal grid cells with a horizontal resolution of 5 km; and D3 is focused on the Porto urban area and has 71 × 91 horizontal grid cells with a horizontal resolution of 1 km. The vertical grid was composed of 30 vertical layers up to the top of the computational domain (50 hPa). The two-way nesting technique was applied for the simulations (Skamarock et al., 2008). According to previous studies conducted over Portugal (Coelho et al., 2020; Ferreira et al., 2020; Rafael et al., 2020b), the following combination of physical parameterizations was selected: i) the microphysics (grid-scale clouds) was resolved using the WRF single moment 5-class scheme (Hong and Lim, 2006); ii) the radiation schemes included the Dudhia shortwave radiation scheme (Dudhia, 1989) and the RRTM (Rapid Radiative Transfer Model) longwave radiation scheme (Mlawer et al., 1997); iii) the

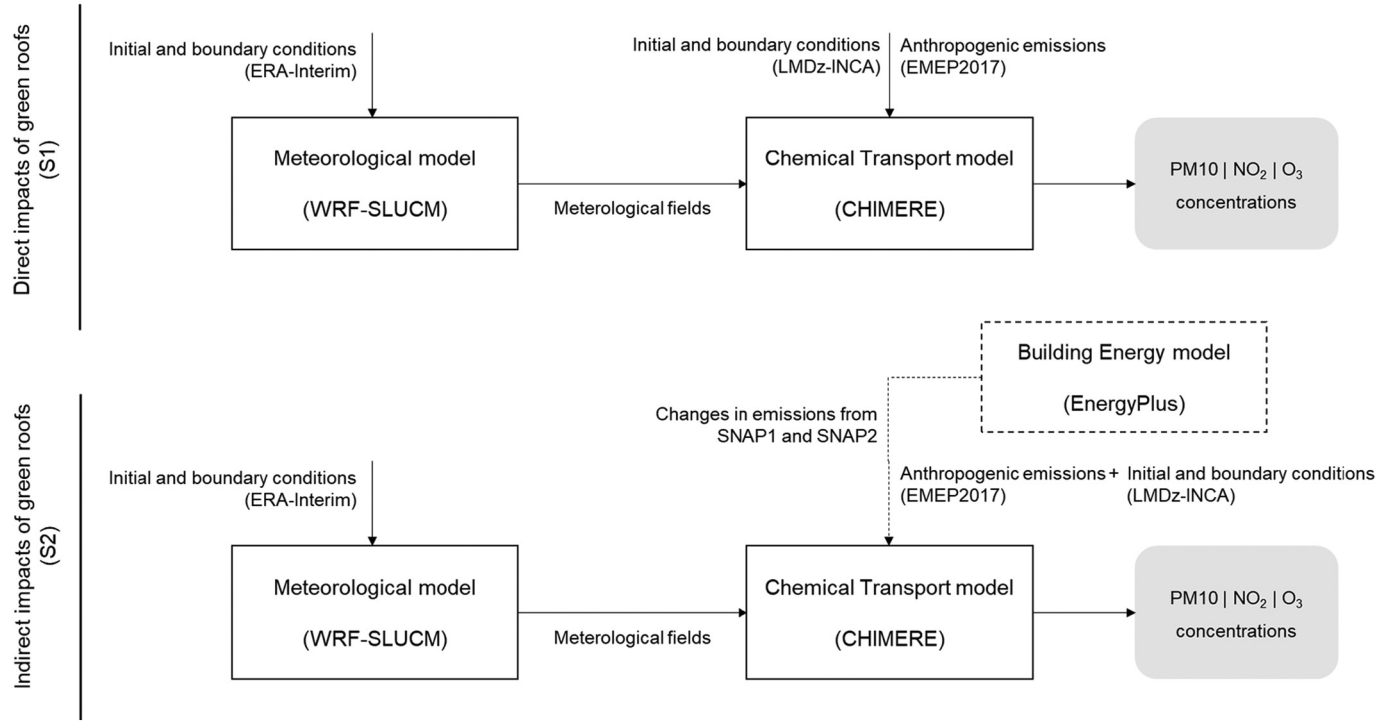

Fig. 1. Schematic representation of the methodology applied to assess the direct (S1) and indirect (S2) impacts of green roofs in the Porto urban area.

Planetary Boundary Layer was resolved by the Yonsei University (YSU) scheme (Hong et al., 2006); iv) the cumulus parameterization scheme (subgrid-scale convective clouds) for lower resolution domains (D1 and D2) were parameterized by the new Grell scheme (Grell, 1993; Grell and Devenyi, 2002); and v) the land surface was resolved by the four-layer Noah land surface model (Tewari et al., 2004).

The meteorological initial and boundary conditions for the coarse domain (D1) were obtained from the European Centre for Medium-Range Weather Forecasts (ECMWF) *Re*-Analysis Interim (ERA-Interim) model data (http://www.ecmwf.int/en/research/climate-reanalysis/era-interim) with 1° × 1° spatial resolution and temporal resolution of 6-h for surface and pressure levels. For the other domains, the initial and boundary conditions came from the respective parent domain. The sea surface temperatures and the soil moisture were also initialized using the ECMWF data.

To better detail Porto's urban features, a complementary approach based on the Corine Land Cover project 2006 version (CLC2006, Büttner et al., 2006), with a 3 arc-seconds horizontal resolution, and on the Porto Urban Atlas from the European Environmental Agency, with 10 m × 10 m of horizontal resolution, was applied. The Porto Urban Atlas was used for the domain areas covered by this database, while CLC2006 was used for areas where such data was not available. Both land-use databases were remapped to the United States Geological Survey (USGS) 33 land use categories following the methodology proposed by Pineda et al. (2004) and Carvalho et al. (2017) described by Rafael et al. (2020a). The USGS 33-category land classification considers 3 different urban classes: low-intensity residential that includes a mixture of 20–70% of vegetation and 30–80% of built-up materials; high intensity residential with built-up materials representing 80–100% and vegetation accounting for less than 20% of the cover; and commercial/industrial/transportation areas, which include infrastructures and the highly developed built-up areas not classified as high-intensity residential. All the remaining areas were considered as non-urbanized areas and as water bodies. The urban categories cover 18.5% of the study domain, with the majority of these areas classified as Low-Intensity Residential (14.2%). The remaining areas are classified as agriculture/forest areas and water bodies. Fig. 2a shows the land use classification in the study area.

The outputs from the WRF model were used as meteorological input data for the CHIMERE model, a state-of-the-art open-access multi-scale Eulerian chemical transport model. CHIMERE computes gas-phase chemistry (Schmidt et al., 2001), aerosol formation, transport and deposition (Bessagnet et al., 2004; Vautard et al., 2005) from continental to urban scales. CHIMERE v2016a1 was applied to the three nested domains presented in Fig. S1. Initial and boundary conditions for the outermost domain were retrieved from The LMDz-INCA (gas species and non-dust aerosols) global chemical-transport model (Hauglustaine et al., 2004). The biogenic emissions were calculated using the online MEGAN model (Model of Emissions of Gases and Aerosols from Nature) (Guenther et al., 2006). The USGS land use data was also used for the air quality simulations. The chemical mechanism MELCHIOR-2 was used to simulate the concentration of 44 gaseous species from a set of 120 chemical reactions; this mechanism is derived from MELCHIOR (Derognat et al., 2003), following the concept of "chemical operators" (Carter, 1990). The dry deposition scheme follows the Wesely parametrizations (Wesely, 1989), which describes dry deposition through a resistance analogy. The Van Leer scheme was used for horizontal advection (Van Leer, 1979). CHIMERE was applied with eight vertical levels; the first layer pressure is 997 mbar (approximately 20 m) and the last extends to 500 mbar.

The atmospheric emissions were obtained from the European Monitoring and Evaluation Programme (EMEP2017). Due to the coarse spatial resolution (0.1° × 0.1°) of this inventory, a top-down methodology (Coelho et al., 2021; Ferreira et al., 2020) was used to improve the horizontal resolution (0.01° × 0.01°) of the atmospheric emissions for the following SNAPs (Selected Nomenclature for Air Pollution): i) SNAP1 – Energy Production – power plants; ii) SNAP5 - extraction and distribution of fossil fuels and geothermal energy; iii) SNAP6 - solvent and other product use; iv) SNAP7 - road transport; v) SNAP8 - other mobile sources and machinery; vi) SNAP9 - waste treatment and disposal; and vii) SNAP10 - agriculture. For SNAP1, the specific location of public power stations was defined in a cell grid of 1 km × 1 km. The approach developed by Silveira et al. (2017), who built a high spatially resolved inventory for the residential combustion sector, provided the required proxy to improve SNAP2 emissions. The OpenStreetMap (OpenStreetMap contributors, 2017) data with the buildings shapes coordinates, and the Transport Emission Model for Line Sources (TREM) (Li et al., 2019; Vicente et al., 2018) were considered, respectively, for the solvent (SNAP 6) and road transport activities (SNAP 7). Finally, the Portuguese land use data (DGT - Direção Geral do Território, 2018), with a spatial resolution of 20 m × 20 m was used to spatially disaggregate emissions of the remaining SNAPs. The information of all SNAPs was then compiled into one file with the same format as the EMEP2017 inventory since this is the format that the CHIMERE emission

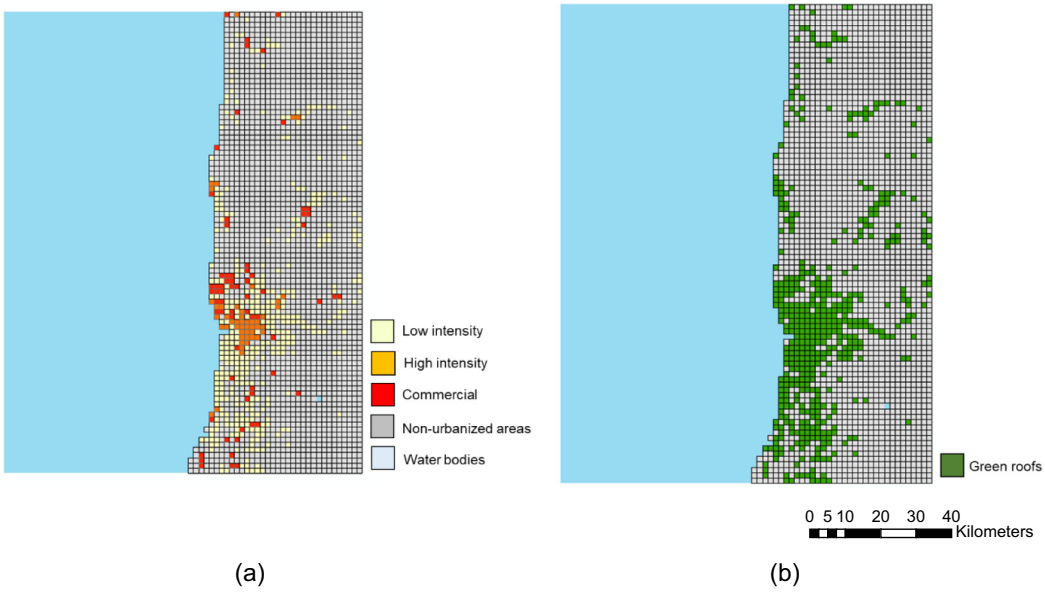

Fig. 2. (a). Land use classification in the Porto urban area – baseline scenario. (b) Location of green roofs considered the green scenarios, which represent 18.5% of the total study area.

pre-processor (EMISURF) is prepared to read. The EMISURF pre-processor temporally disaggregates the emission data using seasonal, weekly and daily profiles, achieving hourly spatially resolved emissions, in a format ready to be read by the CHIMERE model.

This modelling system has been extensively applied worldwide and in Portugal for atmospheric pollution simulations with robust and realistic results (e.g., Ascenso et al., 2020; Rafael et al., 2020a).

3.1.2. Building energy setup

EnergyPlus version 9.1.0 (EnergyPlus Engineering Reference, 2019) was applied to assess the impact of green roofs on building energy needs, as part of the green roof indirect scenario. EnergyPlus is a stand-alone building energy simulation model capable of modelling the hourly energy consumption of a building subject to user-specified environmental and operating conditions (Fantozzi et al., 2021). EnergyPlus includes an eco-roof model option, developed by Sailor (2008), to simulate the effect of a green roof on the modelled building. This enables the user to add a green roof as the outer roof layer on any roof building construction. The model accounts for radiative heat exchange, convective heat transfer, soil heat conductance and storage, and moisture effects. Evapotranspiration from soil and plants is also accounted for. The model requires a set of initial information, which can be divided into the following categories: i) Building location and weather data; ii) Building 3-D model, identifying the building geographical orientation, the location and size of windows and doors, and the climatized and non-climatized zones; iii) Materials and construction configuration of walls, floors, ceilings and windows; iv) Energy loads inside the building (people, lights, electric equipment, etc.), including the schedule and intensity at which these loads are defined; and v) Definition of space type, usage, minimum airflow and shading for each thermal zone, which is calculated internally by the model.

The EnergyPlus model was applied to two kinds of household buildings located in the Porto urban area:

- a typical building configuration, based on the Portuguese Statistics for Construction and Housing (INE – Instituto Nacional de Estatística (Statistics Portugal), 2018), and is characterized by two storeys, each of them with two three-room flats and one one-room flat (with a total area of 191 m^2), and occupation of 7 residents (per storey);
- a tallest building with six storeys with a similar configuration as the typical building, except the sixth storey that is characterized by a three-room flat configuration with 124 m^2 and three residents.

These configurations were chosen due to their predominance in the study area (81% of the total building typologies), which allowed to extrapolate the obtained outcomes from an individual building to the Porto urban area. For both configurations, data related to the materials and construction configuration, energy loads and heating and cooling technology usage were kept constant. The construction elements, such as roof, walls and floor, were obtained from the report of the most used materials in the construction sector in Portugal (OERCO2 - Online Educational Resource for Innovative Study of Construction Materials Life Cycle, 2017). The building's construction elements considered in this study are schematized in Fig. S2 and fully described in the supplementary material. The geometric features and the thermal transmittance of the building components are reported in Table S2 (in the supplementary material).

Two different electric powered utilities were considered for each household building: appliances were defined with a power density of 5 $W{\cdot}m^{-2}$ and lighting at 7 $W{\cdot}m^{-2}$ (Santos, 2017). Both had an operating schedule and usage factor according to the building occupation (variable for weekdays and weekends) and time of the day (Fig. S3a in the supplementary material). The building's occupation was defined with an activity level (Fig. S3b in the supplementary material) and a schedule (Fig. S3c in the supplementary material), variable for weekdays and weekends. Two activity levels were defined (Santos, 2017): i) sleeping, represented by a sensible heat load of 77.1 $W{\cdot}person^{-1}$; and ii) standing with medium level activity, with a sensible heat load of 180 $W{\cdot}person^{-1}$. A fresh air rate of 0.0125 $m^3{\cdot}s^{-1}{\cdot}person^{-1}$ was defined when the building is occupied, with a cooling season temperature set point of 25 °C, and 20 °C for the heating season (Santos, 2017).

For the two-building configurations two settings were assumed: i) a typical roof, considering a horizontal roof with white gravel (B1); and ii) an extensive green roof (B2). The extensive green roof was selected in this study since it is appropriate for Porto's climate, and requires fewer installation costs and lower maintenance (compared with intensive green roofs), namely little irrigation needs (Palha and Franca, 2019). A typical 4-layer green roof construction was considered (Fig. S4a in the supplementary material), as described in the supplementary material. Fig. S4b summarizes the physical characteristics of the first layer of each roof in analysis.

3.2. Scenarios description

To allow a complementary, integrated and intercomparison analysis, two green roofs scenarios were defined. The air quality modelling setup was applied for the selected year for the baseline, considering the current urban morphology (BS), and for two green roofs scenarios: scenario 1 (S1) and scenario 2 (S2).

S1 considers that 100% of the urban areas (i.e. the simulation grid cells classified as urban according to the USGS 33-category land use, see Fig. 2b) have green roofs. For that, the green roof system integrated in WRF-SLUCM, as detailed in Yang et al. (2015), was activated. The green roof system, when compared to conventional roofs, adds three layers; vegetation-soil, growing media and drainage layer. Table 1 summarizes the physical parameters considered in the analysis. It should be noted that since the SLUCM considers a spatial average of each urban grid cell, no distinction is made among individual buildings within each urban grid cell (Li et al., 2014). Thus, this fraction of green roofs implies that 100% of buildings within the grid cell are covered by green roofs while 0% of the buildings are covered by conventional roofs. This scenario implies that changes in air quality data are only related to changes in the meteorological variables, according to the linkages between meteorology and air quality. S1 assesses the direct benefits of green roofs in both climate and air quality nexus.

S2 also considers that 100% of urban areas are covered with green roofs but aims to assess the indirect benefits of green roofs. The goal is to investigate the impacts of green roofs on local air quality by combining the effects related to changes in the meteorological variables with the effects in atmospheric emissions, resulting from changes in the buildings energy needs. The S2 assessment comprises three steps: 1) application of EnergyPlus model to explore the effects of green roofs on the buildings' energy needs, according to the methodology described in Section 3.1.2; 2) analysis of green roofs impacts in terms of environmental and economic indicators (based on the carbon dioxide emissions avoided and on energy savings, respectively); step 2 also includes the recalculation of EMEP emission inventory for the Porto urban area, due to the impact of green roofs on the energy demand for heating and cooling purposes; 3) application of WRF-SLUCM-CHIMERE to assess local air quality, following the methodology described in Section 3.1.1.

The environmental and economic effects of green roofs were explored individually, for each building configuration in analysis, and extrapolated to the Porto urban area, to give an insight into the potential of green roofs at the city level. The CO_2 emissions related to the building energy needs for each building configuration and type of roof (B1 and B2) were estimated considering the energy usage by energy source (electricity, natural gas, wood, and LPG) and the related emission factor (Eq. (1)).

$$CO2_{emission}[tCO_2] = Energy\ usage_{source}\ [MWh/y] \times Emission\ Factor_{source}[tCO_2/MWh] \quad (1)$$

Table 1
Main features of the simulations performed. The abbreviations are defined as follow: GR_FLAG - Activated/disabled the green roof option; GR_TYPE - Type of vegetation in the green roofs; GR_FRAC_ROOF - Fraction of green roof over the roof.

	Simulations		
	Baseline Scenario (BS)	Scenario 1 (S1)	Scenario 2 (S2)
Simulated period		1-Year (2017)	
Meteorological urban physics		SLUCM	
Green roof parameters			
GR_FLAG	0 - Green roof option deactivated	1 - Green roof option activated	1 - Green roof option activated
GR_TYPE	–	2 – Sedum	2 - Sedum
GR_FRAC_ROOF	0	1 (100% of green roof fraction)	1 (100% of green roof fraction)
Anthropogenic emissions	EMEP 2017	EMEP 2017	EMEP 2017 – with changes in emissions from SNAP1 and SNAP2

The usage rate of heating and cooling technology and the related efficiency coefficient (see Table S3 in the supplementary material) were considered to quantify the energy usage. Knowing the CO_2 emission factors related to the energy usage (Table S4 in the supplementary material), the CO_2 emissions avoided with the implementation of a green roof were estimated according to Eq. (2). To extrapolate this knowledge to the Porto urban area, parameters such as the characterization of building configuration over the domain (data obtained from PORDATA (Base de dados Portugal Contemporâneo), 2020b) and household climatization rate (according to Portuguese statistics, INE – Instituto Nacional de Estatística (Statistics Portugal), 2011) were considered. In Porto's study area 78.3% and 22.6% of the households are equipped with heating and cooling devices, respectively, and this information was used for the application of Eq. (3). A similar approach was followed to estimate the costs related to energy savings. Table S4 compiles the emission and cost factors used in this assessment.

$$CO2\ avoided[\%] = \left(\frac{Emission_{buildings\ (B2)} - Emission_{buildings\ (B1)}}{Emission_{buildings\ (B1)}}\right) * 100\% \quad (2)$$

$$Total_{emission}[tCO_2] = N_{buildings} \times \sum_{i=1}^{n_{sources}} CO2\ emission \quad (3)$$

The recalculation of EMEP emission inventory for the Porto urban area was focused on the sectors where there is a direct link between energy consumption and atmospheric emissions: the energy production sector (SNAP1) and the commercial and residential combustion activity sector (SNAP2). The estimation of atmospheric emissions due to energy changes, by pollutant *p*, were quantified applying Eqs. (4) and (5).

$$Green\ roof\ emissions_{p,f,t,i}\ [ton] = Nbuildings \times Energy\ saving \times Fuel_f \times Technology_t \times EF_p \quad (4)$$

$$Emissions_{p,i}\ [ton] = EMEP_{p,i}(baseline) - \sum Green\ roof\ emissions_{p,f,t,i} \quad (5)$$

Three kinds of data were needed: i) the number of buildings by typology in the Porto parishes (Nbuildings), obtained from the National Institute of Statistics, and their spatial distribution by grid cell *i* (with 1 km × 1 km of horizontal resolution), which was improved using the Portuguese census data by neighbourhood (see Fig. S5 in the supplementary material); ii) the percentage of each technology *t* used for heating/cooling needs, obtained from Table S3 data, and percentage of fuel *f* (LPG, natural gas, gas oil and wood) used by each technology, that was quantified using the information of the Portuguese informative inventory report 1990–2017 (APA - Agência Portuguesa do Ambiente, 2019); iii) emission factors (EF) for each atmospheric pollutant *p*, obtained from Tables S5 and S6. For SNAP2, the changes in atmospheric emissions were spatially applied according to the energy saved by each building type (based on the spatial distribution and total number), through the application of Eqs. (4) and (5) and using the data from Tables S3 and S5. For SNAP1, the impact of green roofs on emissions was only considered in the largest Power Plant located within the study area, where the main fuel used is Natural Gas, based on the emission factors from Table S6 and applying Eqs. (4) and (5).

For a more comprehensible analysis of the proposed scenarios, the main features considered in each of them are provided in Table 1.

4. Results and discussion

The direct (Section 4.1) and indirect (Section 4.2) benefits of green roofs in the Porto urban area's air quality, along a full meteorological year (2017), are displayed and discussed. The assessment was performed based on a co-benefit approach: i) Section 4.1 explores the climate-air quality nexus, providing a meteorological and air quality analysis; ii) Section 4.2 explores the effects of the green roof on buildings energy consumption for heating/cooling and implications in atmospheric emissions, costs, and air quality.

4.1. Direct benefits

To evaluate the direct effects of green roofs on air quality, their influence on meteorological variables was firstly investigated. The meteorological variables were selected based on their importance to the thermal performance of buildings, their recognized influence on air quality modelling, and knowledge learned in previous works (e.g., Rafael et al., 2020a; Fallmann et al., 2016). Variables such as 2 m temperature (T2), 10 m wind velocity (U10), planetary boundary layer height (PBLH), latent heat flux (LH) and sensible heat flux (HFX) were used for this analysis. This information was directly obtained from the WRF-SLUCM application. For the analysis of the direct benefits of green roofs in the selected meteorological variables three different approaches were adopted: i) mapping of monthly averages differences between the green roof scenario (S1) and the baseline scenario (BS) results (Fig. 3), to understand the spatial and seasonal variability of the meteorological variables; ii) calculation of the absolute monthly differences between the S1 and the BS results for the region as a whole (Table S7 in the supplementary material), to assess the averaged behaviour of the study area and to have a global perspective of how green roofs influence the meteorology of the urban region; and iii) delivery of daily and monthly profiles based on the differences between S1 and BS results for each type of built-up land use (using a weighted average) (Fig. 4), to explore how the results are influenced by land use.

Looking at the spatial effects of green roofs in the air temperature of Porto urban area for the year 2017 (Fig. 3), two main conclusions can be drawn: i) distinct behaviours were obtained according to the season, with green roofs increasing the average air temperature in the autumn and winter seasons (October to March) and decreasing it in the spring and summer seasons (April to September); ii) similar spatial patterns were obtained through the year, with the magnitude of the differences varying according to the month in analysis, and with higher differences (positive or negative) being obtained in more densely built-up areas (the magnitude of differences increases as more pronounced is the level of urbanization). As shown in Table S7, alike behaviour was obtained for the planetary boundary layer height, with the green roofs

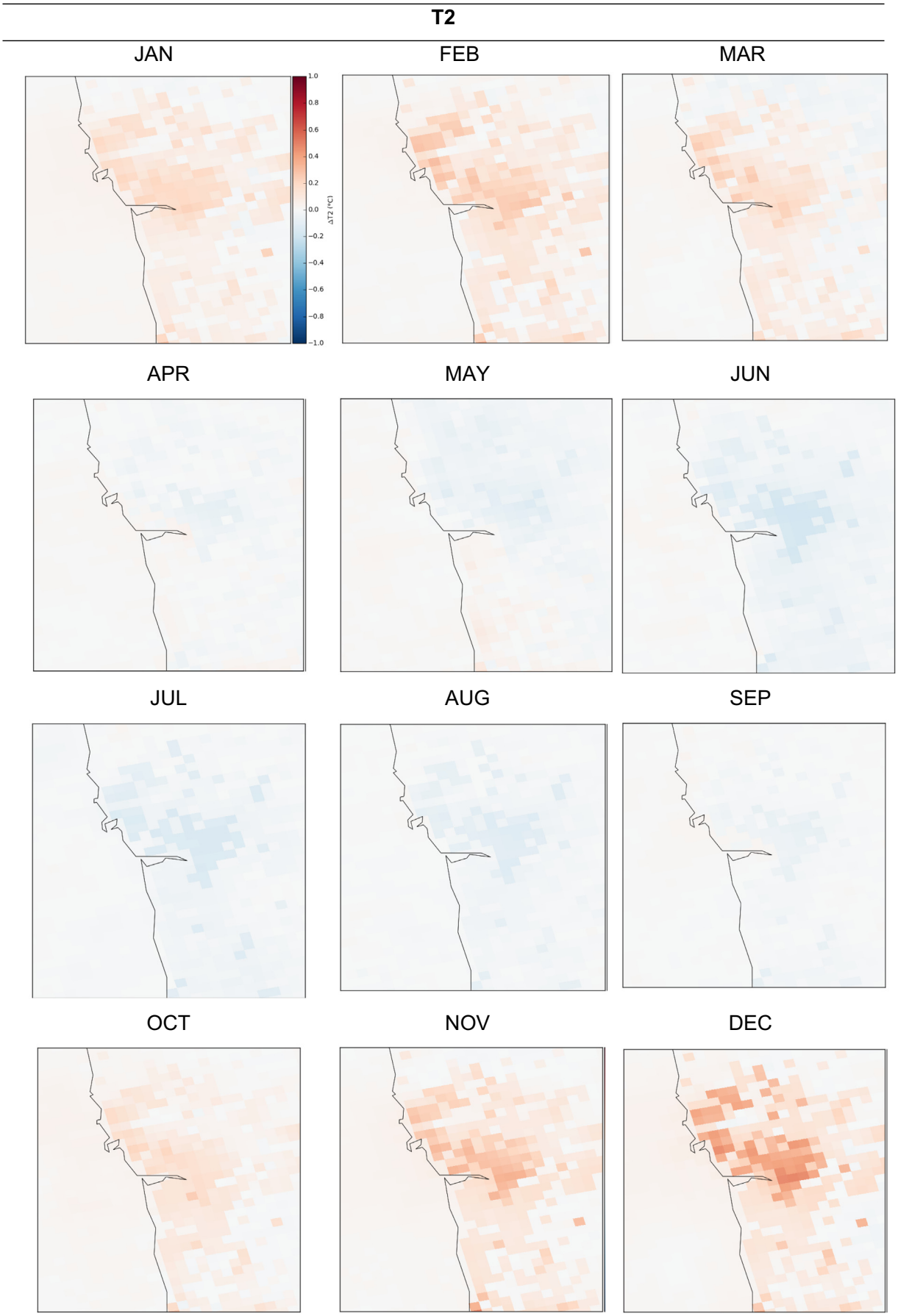

Fig. 3. Spatial distribution of the absolute differences between the green roof scenario (S1) and the baseline scenario (BS) results for temperature (°C) at 2 m. The differences are presented as a monthly average.

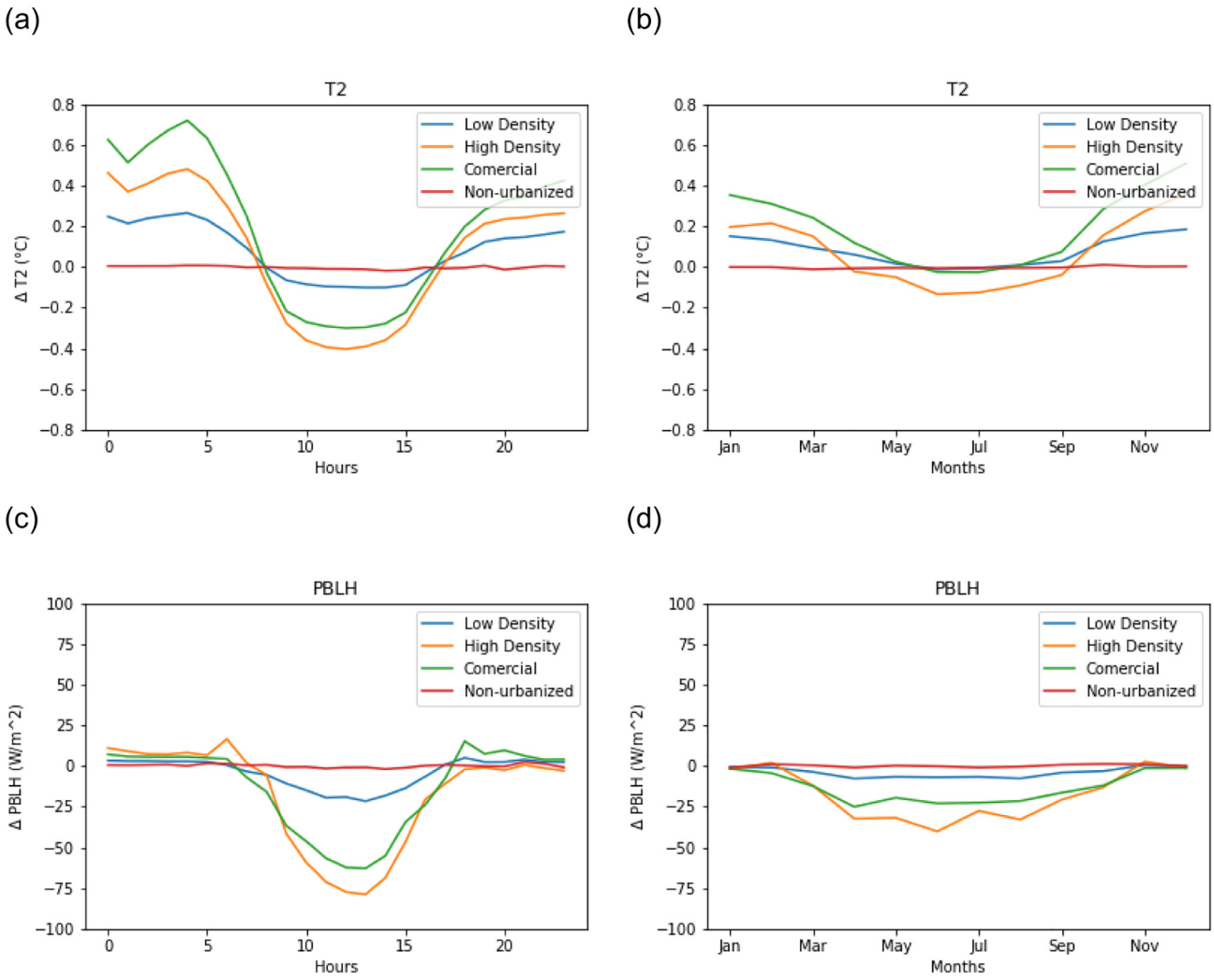

Fig. 4. (a, c) Daily and (b, d) monthly average differences (absolute values) of air temperature (T2) and boundary layer height (PBLH), considering a spatial average by land use category: built-up areas (low-intensity residential, high-intensity residential, and industrial or commercial) and non-urbanized areas.

promoting an overall decrease of the boundary layer height in the spring and summer seasons, and a slight increase in the autumn and winter seasons. A distinct behaviour was found for the turbulent heat fluxes: the latent heat flux increased in all seasons with the implementation of green roofs, with more pronounced differences in summer and spring seasons; whereas an overall decrease of sensible heat flux was obtained, which was higher for summer and spring (see Table S7) and residual in the winter months. There were no effects on the mean wind velocity along the year (results not shown).

The spatial-temporal (monthly) averages of temperature differences were always lower than 0.5 °C, with a maximum reduction being obtained in June (−0.9 °C) (see Table S7). The cooling effects were more pronounced in summer (average differences of 1.5%) than spring (average differences of 1.2%), on sunny days than rainy and cloudy days, and at night than in the daytime. In the cold period (autumn and winter months), the maximum warming effect was obtained in January and December, with a value of +1.98 °C. Overall, the magnitude of the differences was higher in the cold period (overall differences of 12.5%) than in the warmer months (overall differences of 1.4%). This can be explained by the cold climate conditions that occurred in Portugal in 2017, when an average temperature lower 0.8 °C and a minimum temperature lower 1.9 °C than the normal values (1971–2000) were recorded (IPMA - Instituto Português do Mar e da Atmosfera (Meterology Institute), 2018).

These results are related to green roofs' ability to work as insulator and temperature buffer, promoting a decrease of high surface temperatures (Wong et al., 2007) and smoothing low winter temperatures (Teemusk and Mander, 2010). The potential of green roofs to decrease urban temperatures and mitigate the urban heat island effect has been shown in previous works (Carvalho et al., 2017; Solcerova et al., 2017; Rafael et al., 2020a). The cooling effects of green roofs are related to their capability to sustain a large evapotranspiration rate, which is augmented by high solar radiation combined with high air temperatures (Rafael et al., 2016). The increase of evapotranspiration rate implies a change of the atmosphere-surface exchanges by enhancing the latent heat flux and reducing the magnitude of the sensible heat flux (Rafael et al., 2016) that triggers “cool-island” effects (Santamouris, 2014). In the warmer months, an average decrease in the sensible heat flux of −11.3% (varying between −2.3% in September and −35% in August) was obtained. For the same period, the latent heat flux increases on average +14% (varying between +7% in April and +20% in July). These changes in the surface energy balance have also a direct impact on the planetary boundary layer height since a reduction of the temperature boosts a reduction of the amount of turbulent mixing in the atmosphere, implying a decrease of the PBLH (Fallmann et al., 2016). In the warmer months, the PBLH averaged values decrease (for the average of the domain) between −0.50 m (September) and −1.3 m (April), with maximum differences in July, with a value of −54 m.

In the winter, when vegetation is dormant and evapotranspiration is negligible, the warming effect can be explained by three main features: i) the heat is trapped in the vegetation canopy which augments the near-surface ambient temperature, contributing to reduce the daily temperature variation (Solcerova et al., 2017); ii) the vegetation plays an insulating role and decreases the heat loss through the building roof by reducing convective heat loss between the roof and the atmosphere (Collins et al., 2017; Berardi et al., 2014); and iii) due to the intrinsic link between the latent and sensible heat flux, the reduced latent heat flux in the winter implies an increase of sensible heat flux, which contributes to an increase of the energy released from the ground into the atmosphere. The warming effect obtained in this study has been reported by measurement studies conducted under cold climates (e.g., Peng and Jim, 2015; Collins et al., 2017).

Due to the importance of air temperature and boundary layer height to the air pollutants formation and dispersion, the hourly and monthly differences between the green roof and the baseline scenarios, averaged by typology of land use, were investigated for these variables (Fig. 4).

The analysis of Fig. 4 revealed four main outcomes: i) the majority of the air temperature differences occur at the built-up areas, where the green roofs were implemented, with the non-urbanized areas showing an overall constant and negligible variation throughout the day and the year; ii) the trend of cooling effects at the spring and summer seasons occurred during daytime, between 9 a.m. and 4 p.m., when the shading effect is more pronounced, the thermal transmittance given by the soil is reduced (Gagliano et al., 2015), the evapotranspiration rate is higher and the magnitude of the related latent heat flux increases (Rafael et al., 2016); iii) the magnitude of the cooling effects increases with the level of urbanization, since as higher is the percentage of impervious surfaces, higher is the percentage of green roofs and their related effects; and iv) the winter season experiences warming effects in both day and night time, with the magnitude of the warm effect being higher during the night, early morning and late afternoon, related to the higher temperature differences between the air and ground surface, which increases the transfer of heat to the atmosphere (sensible heat flux).

Regarding the PBLH, a predominant decrease was obtained during daytime, in response to the diurnal cycle of heating and cooling of the surface, as well as throughout the year. This behaviour is a direct response to changes in the thermal interaction between the surface and the atmosphere, which is explained by the reduction of the temperature difference between the ground surface and the atmosphere, promoted by green roofs. Similarly to air temperature, as higher is the level of urbanization, greater was the reduction of turbulent mixing and PBLH under green roofs scenarios. Also, since negligible air temperature variations were obtained in non-urbanized areas, no changes in the PBLH were estimated for those areas.

In a close link to the meteorological variables, Fig. 5 shows the spatial distribution of air quality concentration differences between S1 and BS results, per month.

Three main conclusions can be drawn from the analysis of Fig. 5: i) an increase of the annual average concentrations of primary pollutants – PM10 and NO_2 – was obtained, indicating an overall negative green roof effect, while the annual O_3 concentrations – secondary pollutant – decreases, corresponding to a positive effect; ii) the air pollutants patterns differ along the year, with increases and decreases of the concentration levels; and iii) the impact of green roofs on air quality is slight, with the average monthly differences ranging between -2 $\mu g \cdot m^{-3}$ and $+2$ $\mu g \cdot m^{-3}$. The PM10 and NO_2 differences are higher in the summer and spring months and lower in the winter and autumn months, with the main differences over the highly urbanized areas. Maximum increases of $+3.4$ $\mu g \cdot m^{-3}$ (May) and $+6.3$ $\mu g \cdot m^{-3}$ (June) were estimated for PM10 and NO_2, respectively; and maximum decreases of -5.45 $\mu g \cdot m^{-3}$ for NO_2 and -2.9 $\mu g \cdot m^{-3}$ for PM10 $\mu g \cdot m^{-3}$ (both in November) were obtained. These results are directly explained by the impact of green roofs in the atmospheric dynamics, namely on the boundary layer structure and on the vertical mixing as discussed in the literature (e.g., Rafael et al., 2020a; Arghavani et al., 2019). During the autumn and winter seasons, the increases in air temperature promoted by green roofs implied a slight increase of the PBL height and an increase of the dispersion potential, which boosted a decrease of PM10 and NO_2 concentrations. A reverse effect was obtained in the spring and summer seasons. In those seasons, the green roofs promote a reduction of air temperature and a consequent decrease of the PBLH and the turbulent mixing, with an increase of PM10 and NO_2 concentrations. The differences in the magnitude between PM10 and NO_2 impacts are explained by the dry deposition of PM10 over the surface of the green roof since the increase of the surface roughness increases the deposition velocity, as was discussed by Arghavani et al. (2019). The increase of PM10 deposition promoted by green roofs mitigates the effect of the lower PM10 dispersion. The spatial distribution of the impact on ozone levels varies in a negative correlation with the nitrogen dioxides (NOx) patterns (NO and NO_2), revealing that the obtained differences are mostly an indirect result of the implementation of the green roofs. The ozone differences decrease during the summer and spring seasons, with maximum values of -5 $\mu g \cdot m^{-3}$ (June). This decrease is explained by three main processes (Fallmann et al., 2016; Klein et al., 2014): i) the temperature reduction minimizes the ozone formation; ii) the reduction of the turbulent mixing, due to the PBLH reduction, reduces the downward mixing of ozone from higher levels (ozone concentrations increase with altitude); iii) ozone is removed via NOx titration. In VOC-limited systems, typical of urban areas, O_3 decreases with increasing NOx, mainly in the form of NO. With the implementation of green roofs, NO concentrations increase due to weaker atmospheric turbulence (as the primary pollutants PM10 and NO_2, see Fig. S6 in the supplementary material). During the winter and autumn seasons, the average ozone concentrations increase with green roofs, with maximum differences of $+3.9$ $\mu g \cdot m^{-3}$ (November). This is due to the increase in the PBLH and decrease of NOx, leading to less consumption of O_3 during the night.

In terms of annual averages, the air quality trends reveal that green roofs promote a negative effect on primary pollutants, with an overall increase of PM10 and NO_2 concentrations, and a positive effect on O_3 levels, as they decrease. These conclusions are based on the effects of green roofs on the pollutant's dispersion and deposition only since the ability of green roofs to capture air pollutants was not assessed in this work.

4.2. Indirect benefits

To explore the indirect effects of green roofs on air quality, its influence on the different typologies of buildings was firstly investigated. The analysis consisted of two different approaches: i) monthly analysis of the green roofs impacts on energy consumption for heating and cooling processes; ii) assessment of the implications of energy changes on the environment and economic indicators by type of energy source.

Fig. 6 shows the energy consumption per month for the two buildings typology under analysis with the different roofing systems. The comparison allows evaluating the impact of green roofs on the building's energy consumption during heating and cooling periods.

Results show a decrease in the energy needs for heating and cooling with green roofs, which is more pronounced in the warmer months (cooling needs) and in the typical 2 floors building. In the typical building, with the green roof, the cooling needs decrease in a total of -920.8 $kWh \cdot year^{-1}$ (-23%), with the monthly effect on the cooling demand ranging from a decrease of -34 kWh (October) to -309.4 kWh (July) for the whole building. The heating needs decrease in a total of -258.6 $kWh \cdot year^{-1}$ (-5.7%), with the monthly effect on the heating demand varying from a decrease of -130.7 kWh (January) to an increase of $+28.5$ kWh (April) for the whole building. Similar results were obtained for the tallest building (6 floors), with a total decrease of heating and cooling needs of -197.8 $kWh \cdot year^{-1}$ (-2%), and -415.2 $kWh \cdot year^{-1}$ (-3.9%), respectively. These behaviours agree

with the literature (Castleton et al., 2010; Jaffal et al., 2012; Shafique et al., 2020), highlighting the passive cooling effect of the green roofs during the warmer months, with a constant decrease of cooling needs. In the warmer months, when the solar radiation is relevant, the shading of the vegetation layer and the evapotranspiration phenomena lead to low surface temperatures with consequent impact on the thermal load of the underlying indoor spaces and the surrounding air temperature. In fact, the changes in the surface temperature impact the heat

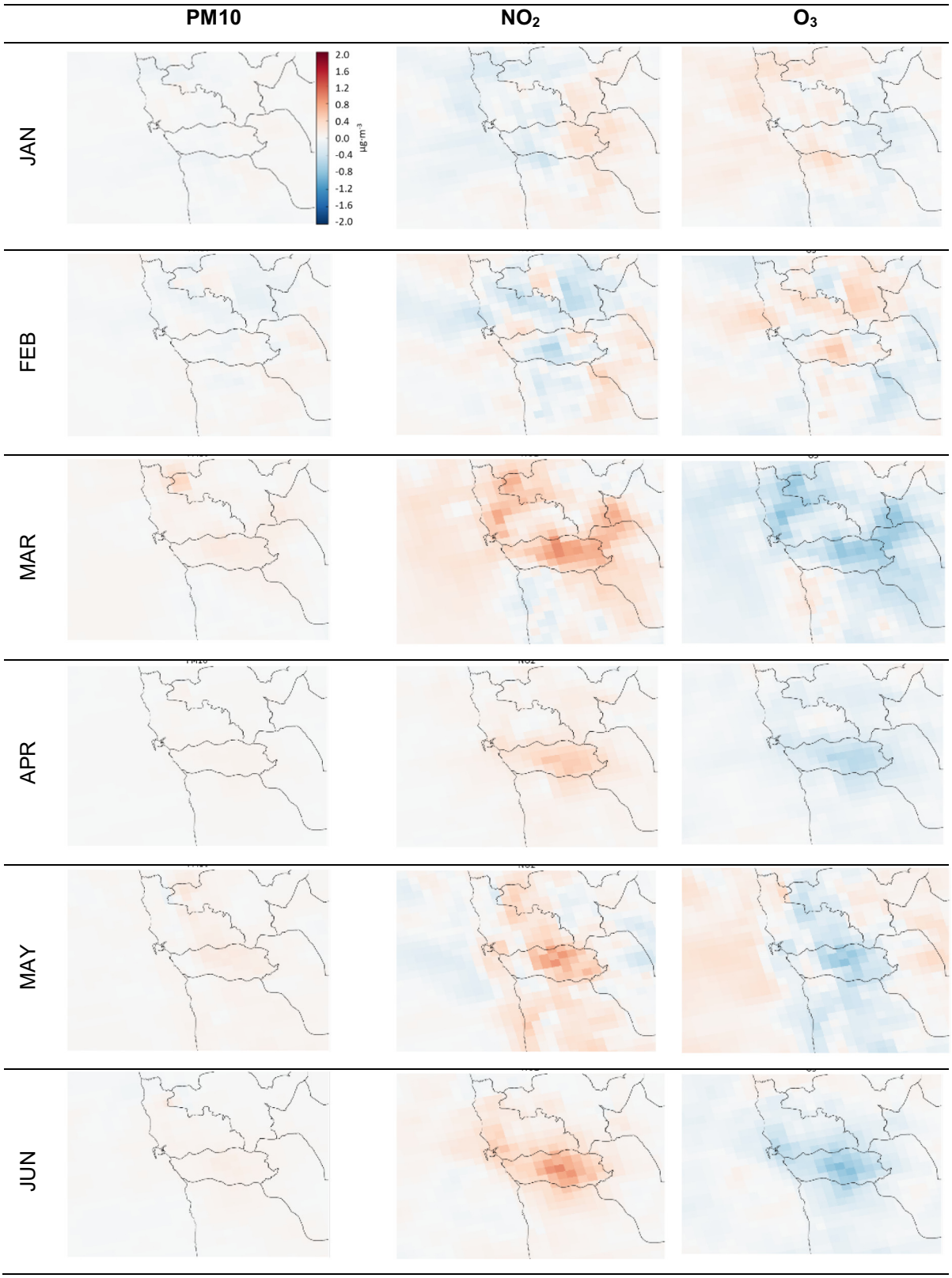

Fig. 5. Spatial distribution of the absolute differences between the green roof scenario (S1) and the baseline scenario (BS) results for PM10, NO_2 and O_3 concentrations. The differences are presented as a monthly average.

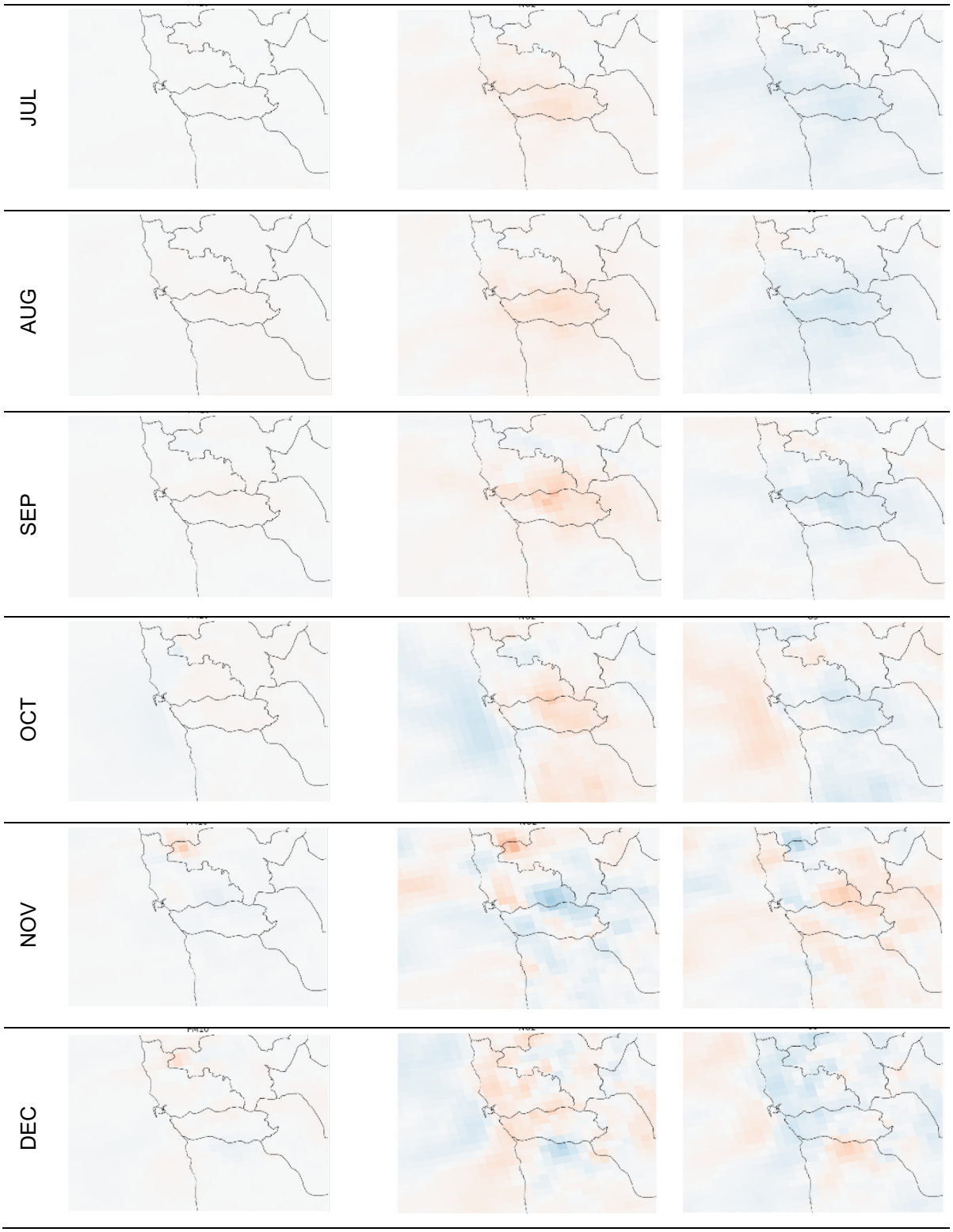

Fig. 5 (*continued*).

flux exchange between the roof and the building's interior, as the indoor air conditions and the energy demand are directly affected by the variation of the heat flux through the roof as a result of green roof usage (Jaffal et al., 2012; Berardi et al., 2014). The differences of the heat flux exchange between the roof and the interior according to the roofing systems are promoted by the fact that green roofs and the typical roofs have different surface albedo and emissivity, which affect the solar radiation and long-wave radiation to the roof surface (Berardi et al., 2014), with the green roof delaying the response of the roof to the radiant heat of the sun (Lin et al., 2013). However, during the cold period, the green roof can increase or decrease the building heating demand, depending on the winter/autumn outdoor conditions and, more importantly, the solar radiation (Jaffal et al., 2012). As explained by Bevilacqua et al. (2018), in the colder months, the elevated difference

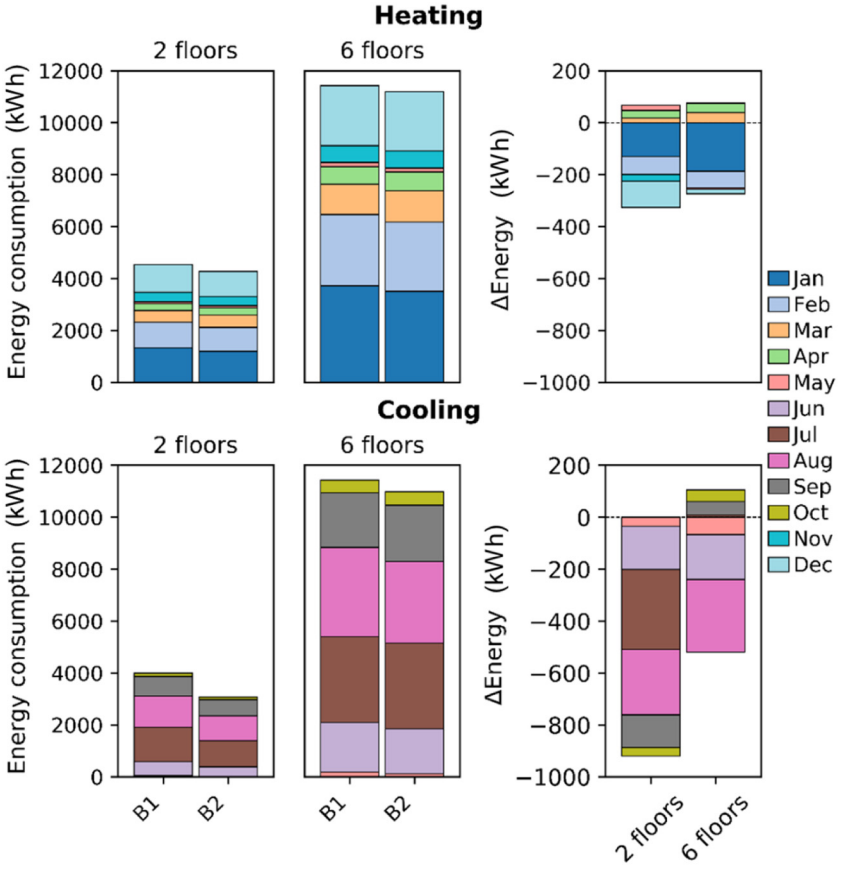

Fig. 6. Monthly energy needs for heating and cooling processes for the configuration of the building (typical two floors building and tallest building - six floors) and the roofing system scenarios (typical roof B1 and extensive green roof B2) in analysis. The monthly energy savings due to green roofs are also shown.

between the steady component of the external surface and indoor air temperature produces a relevant steady heat flux through the envelope. In this case, the thermal capacity does not play a major role.

In a more detailed analysis, the buildings energy consumption by floor was investigated (results not shown). The results revealed that energy savings increase from the ground to the top floor (increase with the proximity to the roof), with the maximum differences being obtained at the top floor for both buildings configuration in analysis. For the typical building, the decrease of the cooling needs ranges between −34.4 kWh (May) and −285.6 kWh (July) on the top floor, with a maximum decrease of −23.7 kWh (July) on the ground floor. This implies an average difference of the energy savings between top and ground floors of 12.7%; maximum differences were obtained in July with the top floor having higher energy savings by 24.7% than the ground floor. The heating needs decreases on average 9.8% on the top floor and 0.8% on the ground floor. For the tallest building, the maximum decreases of the cooling needs occur in August, with values ranging between −30.2 kWh (−8%, ground floor) and −280.9 kWh (−26.7%, top floor), which implies a difference of 18.7%. The heating needs showed similar behaviour, with higher savings being obtained at the top floor, with a reduction of 9.5%.

Fig. 7 turns the improvement of the building's energy performance due to green roofs in environmental (CO_2 emissions avoided) and economic indicators, per building type and for the Porto urban area.

Green roofs promote an overall decrease in CO_2 emissions and costs related to both heating and cooling processes at both building configurations. The energy savings related to the cooling processes boosted a total of 0.09 t and 0.04 t of CO_2 emissions avoided (annual basis) in the typical and tallest buildings, respectively. These energy savings are related to a reduction in the electricity demand due to lesser use of air conditioners, which implied monetary savings of 0.056 k€ and 0.025 k € in the typical and tallest buildings, respectively. This reduction can be supported by two main factors: i) the lack of heat build-up on a green roof implies a decrease in the number of days that air conditioners need to be used for cooling purposes; ii) the ability of green roofs to reduce thermal fluctuations during the day allows the use of air conditioners more efficiently.

For the typical two floors building, the energy savings related to the heating processes boosted a total of 0.05 t of CO_2 emissions avoided (annual basis), varying between −0.008 t CO_2 and −0.04 t CO_2, for natural gas and electricity, respectively. For the tallest building, the avoided CO_2 emissions range between −0.006 t CO_2 and −0.03 t CO_2 for natural gas and electricity, respectively, in a total of 0.04 t of CO_2 emissions avoided. For both typologies of buildings, the electricity was responsible for avoiding 77.6% of the CO_2 emissions, followed by the natural gas and LPG, which contributed to 14.6% and 7.8%, respectively, for the total of CO_2 avoided. These numbers are related to the share of the equipment used for heating purposes. It should be noted that despite no clear consensus among the scientific community on the issue of biomass carbon neutrality, in this study, a neutral CO_2 balance was adopted following the approach of Quinteiro et al. (2020). The authors considered that 'CO_2 in, equals CO_2 out', meaning that the CO_2 released into the atmosphere during the combustion of wood was re-absorbed by the trees during their growing cycle. For that reason, no carbon flux is shown in Fig. 7.

Green roofs can reduce the monetary costs related to the heating and cooling processes. For the cooling processes, a single typical building can save a total of 56.5 €·year^{-1} while a single tallest building can reduce the costs of energy consumption by 25.5 €·year^{-1}. For the heating processes, the electricity consumption was responsible for 55.6% of the

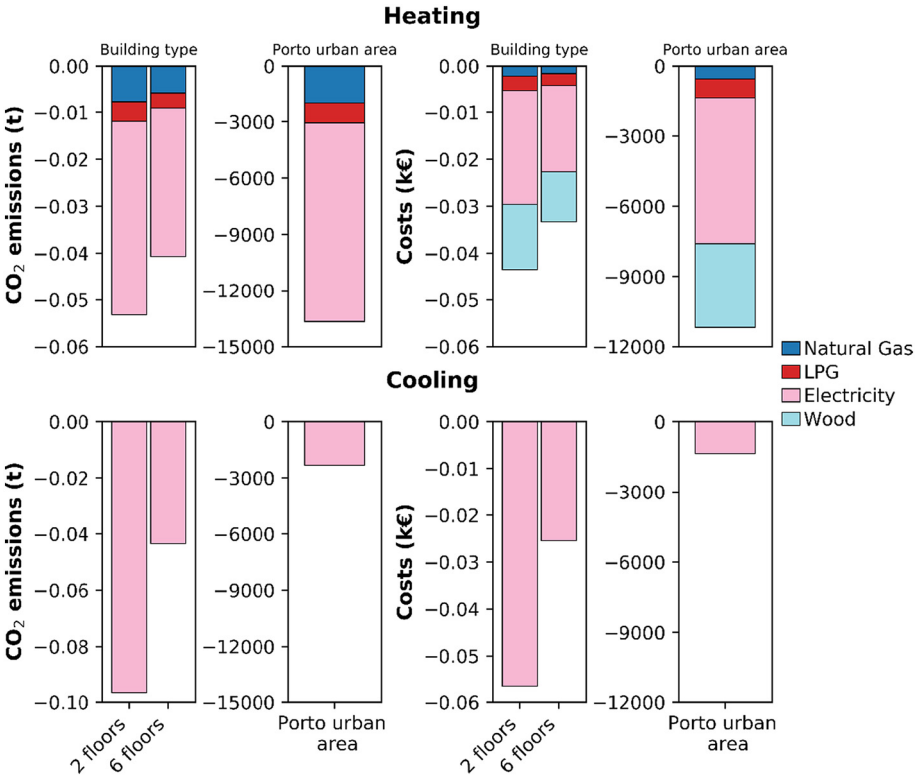

Fig. 7. Environmental (CO_2 emissions) and economic indicators (costs) related to the energy savings promoted by green roofs, for the building's configuration in analysis - typical two floors building and tallest building (six floors). The potential benefits of green roofs in the Porto urban area are also shown.

total monetary savings, in both typologies of buildings, followed by wood in 32%, LPG in 7.5% and natural gas in 4.9%. This distribution is explained by the combined effect between the market price of energy sources applied in Portugal and the share of equipment used for heating purposes. A total monetary saving of 43.6 €·year^{-1} was obtained for a single typical building, varying between −2.1 €·year^{-1} and −24.2 €·year^{-1}, for natural gas and electricity, respectively. For the tallest building, the monetary savings are slightly less, in a total of 33.3 €·year^{-1}.

Looking to a more macroscopic scale – the Porto urban area – the results revealed a potential reduction in the CO_2 emissions of −2332.4 t for cooling and −13,672 t for heating (−1996 t for natural gas, −1070 t for LPG and −10,606 t for electricity), in a total of 16,004 t CO_2 per year (see Fig. 7), which in the same order of magnitude than the results obtained by Mutani and Todeschi (2020). Regarding the costs, it is expected a total monetary saving of 12,549.4 k€·year^{-1}, with the heating processes contributing to a saving of 11,182.9 k €·year^{-1} and the cooling processes contributing with 1366.4 k€·year^{-1}.

Finally, the indirect effects of green roofs on air quality were assessed following two kinds of analysis: i) quantifying the impact of the energy changes promoted by green roofs on the monthly atmospheric emissions; ii) mapping the differences (monthly average) between the green roof scenario (S2) and the baseline results.

Fig. 8 shows the impact of green roofs on atmospheric emissions from the commercial and residential combustion sector (SNAP2) and the energy production sector (SNAP1), on a monthly basis. The results are presented as the difference between S2 and BS.

The results reveal an overall tendency of green roofs to promote reductions in the PM10, PM2.5 and NOx emissions of both activity sectors. Exceptions occurred between March and May, where a slight increase was estimated (less than 10 kt for every pollutant and activity sector). Three main outcomes arise from the analysis of Fig. 8: i) emission reductions from the energy production sector mainly occurred in the warmer months for NOx, with a maximum value of 95.7 kt in July; ii) emission reductions from the commercial and residential combustion sector occurred in the cold period for PM10 and PM2.5 pollutants, with maximum values of 37.5 kt and 36.6 kt in January, respectively; and iii) the changes in the atmospheric emissions (both increases and decreases) are explained by the monthly changes of the energy consumption, as a result of the conjoint influence of the technology used for heating/cooling needs and the fuel used. These results highlight the role of wood combustion in PM10 and PM2.5 emissions and the electricity production from natural gas in NOx emissions.

The total emissions reduction in the energy production sector was −365 kt for NOx and −1.8 kt for PM10 and PM2.5; the reductions in the commercial and residential sector were −11 kt for NOx, −74 kt for PM10 and −72 kt for PM2.5. Despite this positive trend, it should be noted that the obtained reductions represent less than 5% of the total emissions of the Porto urban area. In terms of their spatial distribution (results not shown), the reduction of the energy production sector emissions is limited to the location of the power plant placed within the study domain and its surroundings (in a radius of 1 km), while the reduction of commercial and residential sector emissions is distributed across the study domain within the areas classified as built-up areas.

The implications of the emissions changes on air quality were lastly assessed. The results revealed that the monthly differences between the indirect effect green roof scenario and the baseline scenario have a similar spatial distribution than the differences found for the direct effect (results not shown) but a distinguished trend was observed: an annual average reduction of NO_2 and PM10 concentrations were obtained; for O_3 concentrations an average annual increase was found. Maximum increases of +3.3 μg·m^{-3} (May), +6.8 μg·m^{-3} (June) and +4.4 μg·m^{-3} (February) were estimated for PM10, NO_2 and O_3, respectively; maximum decreases of −5.4 μg·m^{-3} for NO_2 (February), −3.0 μg·m^{-3} for PM10 (November) and −5 μg·m^{-3} (June) were obtained. Comparing S2 and S1, overall, the PM10 and NO_2 concentrations are higher in S1, with average differences of 8% and 4.5%, respectively; due to the decrease of NOx concentrations in S2, a 22.3% averaged increase of O_3

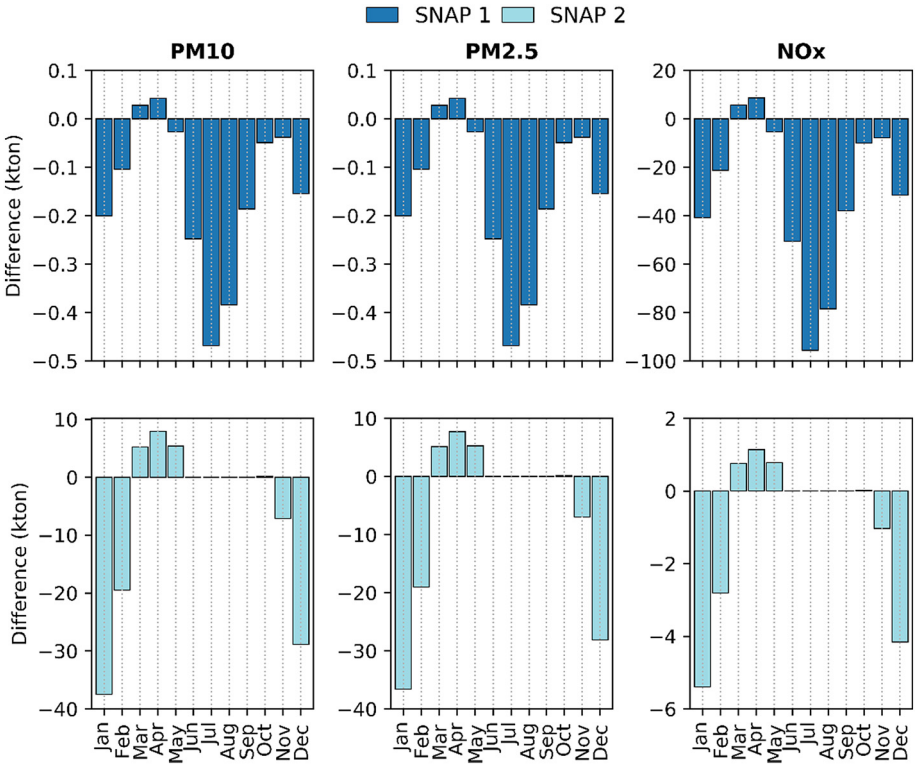

Fig. 8. Implications of the energy savings promoted by green roofs on PM10, PM2.5 and NOx emissions over the Porto urban area.

levels was found in relation to S1. The most prominent differences between S2 and S1 were obtained in the winter season (between December and February) for PM10, highlighting the importance of the residential combustion sector to this pollutant. For NO_2, the highest differences were obtained in August and September. These results indicate that the indirect effects of green roofs (emissions reduction) on the concentrations of primary pollutants does not compensate for the green roofs meteorological impact (direct effect), namely the PBLH reduction, especially in the summer months. Despite the obtained differences, the individual impact of the emissions changes in the PM10, NO_2 and O_3 concentrations were, on an annual average, of around $+/-1$ $\mu g \cdot m^{-3}$.

5. Conclusions

The WRF-CHIMERE coupled with SLUCM modelling system was employed to numerically investigate the direct and indirect effects of green roofs on air quality – PM10, NO_2 and O_3 –, over 1-year (2017) for the Porto urban area. The EnergyPlus model was also used to support the assessment of the indirect impacts through the analysis of buildings energy needs. To do that, a baseline and two green roofs scenarios - S1 and S2 - were defined.

The main outcomes of the current research are summarized as follows:

(a) The effects of green roofs on air temperature vary according to the season. Green roofs increase the average air temperature in the autumn and winter seasons and decrease it in the spring and summer seasons. These data are particularly relevant in the context of climate change, where it is expected an increase of extreme weather events such as heat and cold waves. The spatial distribution does not vary throughout the year, with higher differences occurring in denser urban areas.

(b) Both negative and positive impacts were estimated for the primary and secondary pollutants, respectively, with an overall increase of PM10 and NO_2 annual concentrations, and a decrease of O_3 levels. The results highlight that changes in the urban structure could impact the local meteorological conditions and the boundary layer structure, thermodynamically, which have a key role (through dispersion) in air pollution for the primary pollutants. However, the direct impact of green roofs on air quality is minimal, with maximum monthly differences ranging from -5 to $+5$ $\mu g \cdot m^{-3}$.

(c) The green roofs promote an increase of the buildings energy efficiency, reducing the cooling and heating needs, mainly in the warmer months, in all the buildings typologies under analysis. The changes in the energy consumption had impacts on the environmental and economic indicators of the Porto urban area, with a potential reduction of 16,004 t CO_2 per year and a monetary saving of 12,549.4 k€·year^{-1}. Also, the changes in the energy consumption impacted atmospheric emissions from the energy and commercial and residential sectors, with the results revealing an overall tendency of green roofs to promote reductions in the PM10, PM2.5 and NOx emissions of both activity sectors.

(d) The indirect impact of green roofs on air quality was slight; the emissions changes (by comparing S2 and S1) promoted an impact in PM10, NO_2 and O_3 concentrations of around $-/+1$ $\mu g \cdot m^{-3}$, on average.

It is not the purpose of this paper to provide any kind of recommendation to decision-makers, as different positive and negative effects have to be traded off against each other and more detailed studies are required for such a decision. Anyway, this kind of approach can be applied to other cities and is highly advantageous from a stakeholder's point of view, since it provides information about how the implementation of a specific nature-based solution affects the built-up environment.

CRediT authorship contribution statement

S. Rafael: Conceptualization, Writing – original draft. **L.P. Correia:** Software, Writing – original draft. **A. Ascenso:** Software. **B. Augusto:** Software. **D. Lopes:** Formal analysis, Writing – original draft. **A.I. Miranda:** Supervision, Writing – review & editing.

Declaration of competing interest

The authors Sandra Rafael, Luís P. Correia, Ana Ascenso, Bruno Augusto, Diogo Lopes, and Ana Isabel Miranda would like to declare that there is no conflict of interests.

Acknowledgements

This work was supported by the project GENESIS (PTDC/GES-URB/29444/2017) funded by the Portuguese Science and Technology Foundation through national funds and by the European Community Fund FEDER within the COMPETE2020 program, and by UNaLab project (Grant Agreement No. 730052, Topic: SCC-2-2016-2017: Smart Cities and Communities Nature-based solutions). Thanks are due for the financial support to the PhD grant of A. Ascenso (SFRH/BD/136875/2018), B. Augusto (2020.06293.BD), and CESAM (UIDB/50017/2020+UIDP/50017/2020), to FCT/MCTES through national funds, and the co-funding by the FEDER, within the PT2020 Partnership Agreement and Compete 2020. Thanks are also due to FCT/MCTES for the contract granted to S. Rafael (2020.02543.CEECIND).

Appendix A. Supplementary data

Supplementary data to this article can be found online at https://doi.org/10.1016/j.scitotenv.2021.149313.

References

Alberti, V., Alonso Raposo, M., Attardo, C., Auteri, D., Ribeiro Barranco, R., Batista E Silva, F., Benczur, P., 2019. . ISBN 978-92-76-03847-4 (online), 978-92-76-03848-1 (print). In: Vandecasteele, I., Baranzelli, C., Siragusa, A., Aurambout, J. (Eds.), The Future of Cities. EUR 29752 EN, Publications Office of the European Union, Luxembourg https://doi.org/10.2760/375209 (online)]. JRC116711.

APA - Agência Portuguesa do Ambiente, 2019. Portuguese Informative Inventory Report 1990-2017 Submitted Under the NEC Directive (EU) 2016/2284 and Convention on Long-range Transboundary Air Pollution; Amadora.

Arghavani, S., Malakooti, H., Bidokhti, A., 2019. Numerical evaluation of urban green space scenarios effects on gaseous air pollutants in Tehran Metropolis based on WRF-Chem model. Atmos. Environ. 214, 116832. https://doi.org/10.1016/j.atmosenv.2019.116832.

Ascenso, A., Augusto, B., Silveira, C., Rafael, S., Coelho, S., Monteiro, A., Ferreira, J., Menezes, I., Roebeling, P., Miranda, A.I., 2020. Impacts of nature-based solutions on the urban atmospheric environment: a case study for Eindhoven, The Netherlands. Urban For. Urban Green., 126870 https://doi.org/10.1016/j.ufug.2020.126870.

Berardi, U., GhaffarianHoseini, A., GhaffarianHoseini, A., 2014. State-of-the-art analysis of the environmental benefits of green roofs. Appl. Energy 115, 411–428. https://doi.org/10.1016/j.apenergy.2013.10.047].

Bessagnet, B., Hodzic, A., Vautard, R., Beekmann, M., Cheinet, S., Honoré, C., Rouil, L., 2004. Aerosol modeling with CHIMERE—preliminary evaluation at the continental scale. Atmos. Environ. 38 (18), 2803–2817. https://doi.org/10.1016/j.atmosenv.2004.02.034].

Bevilacqua, P., Mazzeo, D., Arcuri, N., 2018. Thermal inertia assessment of an experimental extensive green roof in summer conditions. Build. Environ. 131, 264–276. https://doi.org/10.1016/j.buildenv.2017.11.033].

Büttner, G., Feranec, G., Jaffrain, G., 2006. Corine land cover nomenclature illustrated guide (Addendum 2006). http://eea.eionet.europa.eu/Members/irc/eionetcircle/spatial/library?l=/clc2005update/clc2006technical/draft/nomenclaturedoc/EN1.0&a=d.

Carvalho, D., Martins, H., Marta-Almeida, M., Rocha, A., Borrego, C., 2017. Urban resilience to future urban heat waves under a climate change scenario: a case study for Porto urban area (Portugal). Urban Clim. 19, 1–27.

Carter, W.P.L., 1990. A detailed mechanism for the gas-phase atmospheric reactions of organic compounds. Atmos. Environ. Part A 24, 481–518. https://doi.org/10.1016/0960-1686(90)90005-8.

Castleton, H.F., Stovin, V., Beck, S.B.M., Davison, J.B., 2010. Green roofs; building energy savings and the potential for retrofit. Energ. Buildings 42, 1582–1591. https://doi.org/10.1016/j.enbuild.2010.05.004.

Chen, F., Kusaka, H., Bornstein, R., Ching, J., Grimmond, C.S.B., Grossman-Clarke, S., Loridan, T., Manning, K.W., Martilli, A., Miao, S., Sailor, D., Salamanca, F.P., Taha, H., Tewari, M., Wang, X., Wyszogrodzki, A.A., Zhang, C., 2011. The integrated WRF/urban modelling system: development, evaluation, and applications to urban environmental problems. Int. J. Climatol. 31, 273–288.

Coelho, S., Rafael, S., Lopes, D., Miranda, A.I., Ferreira, J., 2021. How changing climate may influence air pollution control strategies for 2030? Sci. Total Environ. 758, 143911. https://doi.org/10.1016/j.scitotenv.2020.143911.

Coelho, S., Rafael, S., Coutinho, M., Monteiro, A., Medina, J., Figueiredo, S., Cunha, S., Lopes, M., Miranda, A.I., Borrego, C., 2020. Climate-change adaptation framework for multiple urban areas in northern Portugal. Environ. Manag. 66, 395–406. https://doi.org/10.1007/s00267-020-01313-5.

Collins, S., Kuoppamäki, K., Kotze, D.J., Lü, X., 2017. Thermal behavior of green roofs under Nordic winter conditions. Build. Environ. 122, 206–214. https://doi.org/10.1016/j.buildenv.2017.06.020.

Derognat, C., Beekmann, M., Baeumle, M., Martin, D., Schmidt, H., 2003. Effect of biogenic volatile organic compound emissions on tropospheric chemistry during the atmospheric pollution over the Paris area (ESQUIF) campaign in the Ile-de-France region. J. Geophys. Res. Atmos. 108. https://doi.org/10.1029/2001jd001421].

DGT - Direção Geral do Território, 2018. Cartografia de Uso e Ocupação do Solo (COS, CLC e Copernicus) [WWW Document]. URL. http://www.dgterritorio.pt (accessed 10.19.18).

Dudhia, J., 1989. Numerical study of convection observed during the winter monsoon experiment using a mesoscale two-dimensional model. J. Atmos. Sci. 46, 3077–3107.

EC - European Commission, 2015. Towards an EU Research and Innovation Policy Agenda for Nature-Based Solutions & Re-naturing Cities. Final Report of the Horizon 2020 Expert Group on 'Nature-Based Solutions and Re-Naturing Cities'. Publications Office of the European Union, Luxembourg ISBN 978-92-79-46051-7.

EC - European Commission, 2018. COM/2018/773 Final. Communication From The Commission To The European Parliament, The European Council, The Council, The European Economic And Social Committee, The Committee Of The Regions An d The European Investment Bank: A Clean Planet for All - A European Strategic Long-term Vision for a Prosperous, Modern, Competitive and Climate Neutral Economy.

EC - European Commission, 2019. COM (2019) 640 Final. Communication From The Commission To The European Parliament, The European Council, The Council, The European Economic And Social Committee And The Committee Of The Regions: The European Green Deal.

EEA, European Environmental Agency, 2020. Air quality in Europe 2020 - EEA Report No 09/2020. Publications Office of the European Union, Luxemburg.

EnergyPlus Engineering Reference, 2019. The Reference to EnergyPlus Calculations. US Department of Energy.

EU (European Union) and UN-HABITAT (United Nations Human Settlements Programme), 2016. The State of European Cities 2016. Cities Leading the Way to a Better Future.

Fallmann, J., Forkel, R., Emeis, S., 2016. Secondary effects of urban heat island mitigation measures on air quality. Atmos. Environ. 125, 199–211. https://doi.org/10.1016/j.atmosenv.2015.10.094.

Fantozzi, F., Bibbiani, C., Gargari, C., Rugani, R., Salvadori, G., 2021. Do green roofs really provide significant energy saving in a Mediterranean climate? Critical evaluation based on different case studies. Front. Archit. Res. https://doi.org/10.1016/j.foar.2021.01.006 (in press).

Ferreira, J., Lopes, D., Rafael, S., Relvas, H., Almeida, S.M., Miranda, A.I., 2020. Modelling air quality levels of regulated metals: limitations and challenges. Environ. Sci. Pollut. Res. 27, 33916–33928. https://doi.org/10.1007/s11356-020-09645-9.

Gagliano, A., Detommaso, M., Nocera, F., Evola, G., 2015. A multi-criteria methodology for comparing the energy and environmental behavior of cool, green and traditional roofs. Build. Environ. 90, 71–81. https://doi.org/10.1016/j.buildenv.2015.02.043.

Grell, G.A., 1993. Prognostic evaluation of assumptions used by cumulus parameterization. Mon. Weather Rev. 121, 764–787.

Grell, G.A., Devenyi, D., 2002. A generalized approach to parameterizing convection combining ensemble and data assimilation techniques. Geophys. Res. Lett. 29, 1693. https://doi.org/10.1029/2002GL015311.

Guenther, A., Karl, T., Harley, P., Wiedinmyer, C., Palmer, P.I., Geron, C., 2006. Estimates of global terrestrial isoprene emissions using MEGAN (Model of Emissions of Gases and Aerosols from Nature). Atmos. Chem. Phys. 6, 3181–3210. https://doi.org/10.5194/acp-6-3181-2006.

Hauglustaine, D.A., Hourdin, F., Jourdain, L., Filiberti, M.-A., Walters, S., Lamarque, J.-F., Holland, E.A., 2004. Interactive chemistry in the Laboratoire de Météorologie Dynamique general circulation model: description and background tropospheric chemistry evaluation. J. Geophys. Res. Atmos. https://doi.org/10.1029/2003JD003957.

Hong, S.-Y., Lim, J.-O.J., 2006. The WRF single-moment 6-class microphysics scheme (WSM6). Asia-Pac. J. Atmos. Sci. 42, 129–151.

Hong, S.-Y., Noh, Y., Dudhia, J., 2006. A new vertical diffusion package with an explicit treatment of entrainment processes. Mon. Weather Rev. 134, 2318–2341.

IPMA - Instituto Português do Mar e da Atmosfera (Meterology Institute), 2013. Normais Climatológicas - 1981-2010 (provisórias) (in Portuguese). URL. http://www.ipma.pt/pt/oclima/normais.clima/1981-2010/014/ (accessed: September 2020).

IPMA - Instituto Português do Mar e da Atmosfera (Meterology Institute), 2018. Balanço Climático Preliminar do Ano 2017 Portugal Continental. URL. http://www.ipma.pt/resources.www/docs/im.publicacoes/edicoes.online/20171229/fVhUCTqvyGjAJEZEUlwS/cli_20170101_20171229_pcl_aa_co_pt.pdf (accessed: November 2020).

INE – Instituto Nacional de Estatística (Statistics Portugal), 2018. Estatísticas da Construção e Habitação 2017 ISBN: 978-989-25-0444-5.

INE – Instituto Nacional de Estatística (Statistics Portugal), 2011. Inquérito ao Consumo de Energia no Sector Doméstico 2010 ISBN 978-989-25-0130-7.

Jaffal, I., Ouldboukhitine, S.-E., Belarbi, R., 2012. A comprehensive study of the impact of green roofs on building energy performance. Renew. Energy 43, 157–164. https://doi.org/10.1016/j.renene.2011.12.004.
Kaspersen, P.S., Halsnæs, K., 2017. Integrated climate change risk assessment: a practical application for urban flooding during extreme precipitation. Clim. Serv. 6, 55–64.
Klein, P.M., Hu, X.M., Xue, M., 2014. Impacts of mixing processes in nocturnal atmospheric boundary layer on urban ozone concentrations. Bound.-Layer Meteorol. 150, 107–130. https://doi.org/10.1007/s10546-013-9864-4].
Kusaka, H., Kimura, F., 2004. Thermal effects of urban canyon structure on the nocturnal heat island: numerical experiment using a mesoscale model coupled with an urban canopy model. J. Appl. Meteorol. 43, 1899–1910.
Kusaka, H., Kondo, H., Kikegawa, Y., Kimura, F., 2001. A simple single layer urban canopy model for atmospheric models: comparison with multi-layer and slab models. Bound.-Layer Meteorol. 101, 329–358.
Lalošević, M.D., Komatina, M.S., Miloš, M.V., Rudonja, N.R., 2018. Green roofs and cool materials as retrofitting strategies for urban heat Island mitigation - case study in Belgrade, Serbia. Therm. Sci. 22. https://doi.org/10.2298/TSCI171120086L].
Leal, Filho W., Balogun, A.-L., Olayide, O., Azeiteiro, U.A., Ayal, D.Y., Muñoz, P., Nagy, G.J., Bynoe, P., Oguge, O., Toamukum, N.Y., Saroar, M., Li, C., 2019. Assessing the impacts of climate change in cities and their adaptive capacity: towards transformative approaches to climate change adaptation and poverty reduction in urban areas in a set of developing countries. Sci. Total Environ. 692, 1175–1190. https://doi.org/10.1016/j.scitotenv.2019.07.227.
Li, D., Bou-Zeid, E., Oppenheimer, M., 2014. The effectiveness of cool and green roofs as urban heat island mitigation strategies. Environ. Res. Lett. 9, 055002.
Li, X., Lopes, D., Mo, K.M., Miranda, A.I., Yuen, K.V., 2019. Development of a road traffic emission inventory with high spatial – temporal resolution in the world ' s most densely populated region — Macau. Environ. Monit. Assess. 191, 239. https://doi.org/10.1007/s10661-019-7364-9.
Lin, B.-S., Yu, C.-C., Su, A.-T., Lin, Y.-J., 2013. Impact of climatic conditions on the thermal effectiveness of an extensive green roof. Build. Environ. 67, 26–33. https://doi.org/10.1016/j.buildenv.2013.04.026.
MacIvor, J.S., Margolis, L., Perotto, M., Drake, J.A.P., 2016. Air temperature cooling by extensive green roofs in Toronto Canada. Ecol. Eng. 95, 36–42. https://doi.org/10.1016/j.ecoleng.2016.06.050.
Mlawer, E.J., Taubman, S.J., Brown, P.D., Iacono, M.J., Clough, S.A., 1997. Radiative transfer for inhomogeneous atmospheres: RRTM, a validated correlated-k model for the longwave. J. Geophys. Res. 102D, 16663–16682.
Monteiro, A., Russo, M., Gama, C., Lopes, M., Borrego, C., 2018. How economic crisis influence air quality over Portugal (Lisbon and Porto)? Atmos. Pollut. Res. 9, 439–445. https://doi.org/10.1016/j.apr.2017.11.009.
Mutani, G., Todeschi, V., 2020. The effects of green roofs on outdoor thermal comfort, urban heat island mitigation and energy savings. Atmosphere 11, 123. https://doi.org/10.3390/atmos11020123.
OERCO2 - Online Educational Resource for Innovative Study of Construction Materials Life Cycle, 2017). Study of most used materials in construction sector in Portugal. URL. https://oerco2.eu/wp-content/uploads/2013/02/1.2.1.-Report-Construction-materials-in-Portugal_EN.pdf (accessed: September 2020).
OpenStreetMap contributors, 2017. Planet dump [data file from $date of database dump $]. Retrieved from. https://planet.openstreetmap.org [WWW Document].
Palha, P., Franca, F., 2019. Guia Técnico para Coberturas Verdes - Projeto, Construção e Manutenção. 1a edição. ANCV – Associação Nacional de Coberturas Verdes.
Peng, L.L.H., Jim, C.Y., 2015. Economic evaluation on green-roof environmental benefits in the context of climate change: the case of Hong Kong. Urban For. Urban Green. 14, 554–561. https://doi.org/10.1016/j.ufug.2015.05.006].
Pineda, N., Jorba, O., Jorge, J., Baldasano, J.M., 2004. Using NOAA AVHRR and SPOT VGT data to estimate surface parameters: application to a mesoscale meteorological model. Int. J. Remote Sens. 25, 129–143. https://doi.org/10.1080/01431160310001152011.
PORDATA (Base de dados Portugal Contemporâneo), 2020a. Consumo de energia final e de energia eléctrica pelo sector doméstico (%) [Electrical energy consumption: total and by type of consumer sector]. URL. https://www.pordata.pt/Europa/Consumo de energia final e de energia el%C3%A9ctrica pelo sector dom%C3%A9stico (percentagem)-1734 (accessed: September 2020).
PORDATA (Base de dados Portugal Contemporâneo), 2020b. Edifícios segundo os Censos: total e por número de pisos [Buildings, according to the Census: total and by number of floors]. URL. https://www.pordata.pt/Municipios/Edif%c3%adcios segundo os Censos total e por n%c3%bamero de pisos-85 (accessed: September 2020).
Quinteiro, P., Greco, F., Tarelho, L.A.D., Righi, S., Arroja, L., Dias, A.C., 2020. cA comparative life cycle assessment of centralised and decentralised wood pellets production for residential heating. Sci. Total Environ. 730, 139162. https://doi.org/10.1016/j.scitotenv.2020.139162.
Rafael, S., Martins, H., Sá, E., Carvalho, D., Borrego, C., Lopes, M., 2016. Influence of urban resilience measures in the magnitude and behaviour of energy fluxes in the city of Porto (Portugal) under a climate change scenario. Sci. Total Environ. 566–567, 1500–1510. https://doi.org/10.1016/j.scitotenv.2016.06.037.
Rafael, S., Vicente, B., Rodrigues, V., Miranda, A.I., Borrego, C., Lopes, M., 2018. Impacts of green infrastructures on aerodynamic flow and air quality in Porto's urban area. Atmos. Environ. 190, 317–330. https://doi.org/10.1016/j.atmosenv.2018.07.044.
Rafael, S., Rodrigues, V., Fernandes, A.P., Augusto, B., Borrego, C., Lopes, M., 2019. Evaluation of urban surface parameterizations in WRF model using energy fluxes measurements in Portugal. Urban Clim. 28, 100465. https://doi.org/10.1016/j.uclim.2019.100465].
Rafael, S., Augusto, B., Ascenso, A., Borrego, C., Miranda, A.I., 2020a. Re-naturing cities: evaluating the effects on future air quality in the city of Porto. Atmos. Environ. 222, 117123. https://doi.org/10.1016/j.atmosenv.2019.117123.
Rafael, S., Martins, H., Matos, M.J., Cerqueira, M., Pio, C., Lopes, M., Borrego, C., 2020b. Application of SUEWS model forced with WRF: energy fluxes validation in urban and suburban Portuguese areas. Urban Clim. 33, 100662. https://doi.org/10.1016/j.uclim.2020.100662.
Sá, E., Martins, H., Ferreira, J., Marta-Almeida, M., Rocha, A., Carvalho, A., Freitas, S., Borrego, C., 2016. Climate change and pollutant emissions impacts on air quality in 2050 over Portugal. Atmos. Environ. 131, 209–224. https://doi.org/10.1016/j.atmosenv.2016.01.040].
Sadineni, S.B., Madala, S., Boehm, R.F., 2011. Passive building energy savings: a review of building envelope components. Renew. Sust. Energ. Rev. 15, 3617–3631. https://doi.org/10.1016/j.rser.2011.07.014.
Sailor, D.J., 2008. A green roof model for building energy simulation programs. Energ. Buildings 40, 1466–1478. https://doi.org/10.1016/j.enbuild.2008.02.001].
Santamouris, M., 2014. Cooling the cities – a review of reflective and green roof mitigation technologies to fight heat island and improve comfort in urban environments. Sol. Energy 103, 682–703. https://doi.org/10.1016/j.solener.2012.07.003].
Santos, A., 2017. Avac Um Manual de Apoio Fundamentos. ISBN: 9789897232503. URL. Volume 1. (PT). Publindústria. https://www.bertrand.pt/livro/avac-um-manual-de-apoio-fundamentos-volume-1-antonio-jose-da-anunciada-santos/20914129.
Schmidt, H., Derognat, C., Vautard, R., Beekmann, M., 2001. A comparison of simulated and observed ozone mixing ratios for the summer of 1998 in Western Europe. Atmos. Environ. 35, 6277–6297. https://doi.org/10.1016/S1352-2310(01)00451-4].
Shafique, M., Xue, X., Luo, X., 2020. An overview of carbon sequestration of green roofs in urban areas. Urban For. Urban Green. 47, 126515. https://doi.org/10.1016/j.ufug.2019.126515.
Silveira, C., Ferreira, J., Monteiro, A., Miranda, A.I., Borrego, C., 2017. Emissions from residential combustion sector: how to build a high spatially resolved inventory. Air Qual. Atmos. Health 1–12. https://doi.org/10.1007/s11869-017-0526-4].
Skamarock, W.C., Klemp, J.B., Dudhia, J., Gill, D.O., Barker, D.M., Huang, X.Y., Wang, W., Powers, J.G., 2008. A Description of the Advanced Research WRF Version 3. NCAR/TN-475 STR, p. 113.
Solcerova, A., van de Ven, F., Wang, M., Rijsdijk, M., van de Giesen, N., 2017. Do green roofs cool the air? Build. Environ. 111, 249–255. https://doi.org/10.1016/j.buildenv.2016.10.021].
Teemusk, A., Mander, Ü., 2010. Temperature regime of planted roofs compared with conventional roofing systems. Ecol. Eng. 36, 91–95. https://doi.org/10.1016/j.ecoleng.2009.09.009.
Tewari, M., Chen, F., Wang, W., Dudhia, J., LeMone, M.A., Mitchell, K., Ek, M., Gayno, G., Wegiel, J., Cuenca, R.H., 2004. Implementation and verification of the unified NOAH land surface model in the WRF model. Paper 14.2A, 20th Conference on Weather Analysis and Forecasting/16th Conference on Numerical Weather Prediction. Vol. 1115 , p. 6. https://ams.confex.com/ams/pdfpapers/69061.pdf.
Van Leer, B., 1979. Towards the ultimate conservative difference scheme, V A second order sequel to Godunov's method. J. Comput. Phys. 32, 101–136. https://doi.org/10.1016/0021-9991(79)90145-1].
Vautard, R., Honoré, C., Beekmann, M., Rouil, L., 2005. Simulation of ozone during the August 2003 heat wave and emission control scenarios. Atmos. Environ. 39, 2957–2967. https://doi.org/10.1016/j.atmosenv.2005.01.039.
Vicente, B., Rafael, S., Rodrigues, V., Relvas, H., Vilaca, M., Teixeira, J., Bandeira, J., Coelho, M., Borrego, C., 2018. Influence of different complexity levels of road traffic models on air quality modelling at street scale. Air Qual. Atmos. Health 11, 1217–1232. https://doi.org/10.1007/s11869-018-0621-1.
Wesely, M.L., 1989. Parameterization of surface resistances to gaseous dry deposition in regional-scale numerical models. Atmos. Environ. 23, 1293–1304. https://doi.org/10.1016/0004-6981(89)90153-4.
Wong, N., Tan, P., Chen, Y., 2007. Study of thermal performance of extensive rooftop greenery systems in the tropical climate. Build. Environ. 42, 25–54. https://doi.org/10.1016/j.buildenv.2005.07.030.
Yang, J., Wang, Z.-H., Chen, F., Miao, S., Tewari, M., Voogt, J.A., Myint, S., 2015. Enhancing hydrologic modelling in the coupled weather research and forecasting - urban modelling system. Bound.-Layer Meteorol. 155, 87–109.